Supporting Information

for

Ionic mesoporous polyamide enabling highly dispersive ultrafine Ru nanoparticles: synergistic stabilization effect and remarkable efficiency in levulinic acid conversion into γ-valerolactone

Qian Wang, Xingchen Ling, Tingting Ye, Yu Zhou*, Jun Wang*

State Key Laboratory of Materials-Oriented Chemical Engineering, College of Chemical Engineering, Nanjing Tech University, Nanjing, 210009, China

*Corresponding author

E-mail: njutzhouyu@njtech.edu.cn (Y. Zhou); junwang@njtech.edu.cn (J. Wang).

Supplementary Experimental

1. Synthesis of carboxylic functional ionic monomers

Synthesis of DNph (Scheme S1): Nicotinic acid (1.24 g, 10 mmol) and α,α'-dichloro-*p*-xylene (0.96 g, 5.5 mmol) were dissolved in acetonitrile (30 mL) at 95 °C and then stirred for 24 h. The emerged white solid was isolated by filtration, washed with acetonitrile and dried at 50 °C for 12 h to give the final product DNph (1.54 g, 73% yield).Found: N, 6.58%; C, 56.06%; H, 4.361%; on theory: N, 6.64%; C, 57.02%; H, 4.30%.

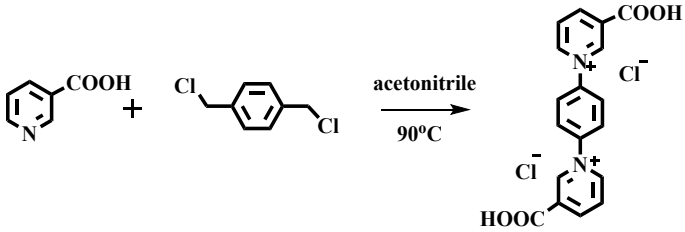

Scheme S1. Synthesis of 1,4-bis[(3-carboxypyridino)methyl]-phenyl dichloride (DNph).

Synthesis of DNph$_2$ (Scheme S2): Nicotinic acid (1.24 g, 10 mmol) and 4,4'-bis(chloromethyl)bipheny (1.38 g, 5.5 mmol) were dissolved in acetonitrile (30 mL) at 95 °C and then stirred for 24 h. The emerged white solid was isolated by filtration, washed with acetonitrile and dried at 50 °C for 12 h to give the final product DNph$_2$ (1.77 g, 71% yield). Found: N, 5.51%; C, 61.40%; H, 4.55%; on theory: N, 5.63%; C, 62.78%; H, 4.46%.

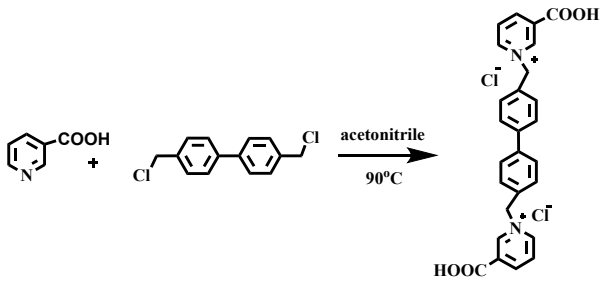

Scheme S2. Synthesis of 4,4′-bis[(4-carboxypyridino)methyl]-biphenyl dichloride (DNph$_2$).

Synthesis of TNph (Scheme S3):Nicotinic acid (0.868 g, 7 mmol) and 1,3,5-tris(bromomethyl)benzene (0.707 g, 2 mmol) were dissolved in acetonitrile (30 mL) at 95 °C and then stirred for 24 h. The emerged white solid was isolated by filtration, washed with acetonitrile and dried at 50 °C for 12 h to give the final product TNph (1.13 g, 78% yield). Found: N, 5.71%; C, 44.21%; H, 3.37%; on theory: N, 5.79%; C, 44.65%; H, 3.33%.

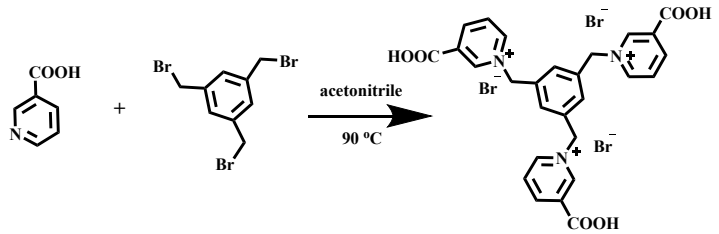

Scheme S3. Synthesis of 1,3,5-tris[(3-carboxypyridino)methyl]-phenyl tribromide (TNph).

Synthesis of TIph (Scheme S4): Isonicotinic acid (1.24 g, 10 mmol) and 1,3,5-Tris(bromomethyl)benzene (1.96 g, 5.5 mmol) were dissolved in acetonitrile (30 mL) at 95 °C and then stirred for 24 h. The emerged white solid was isolated by filtration, washed with acetonitrile and dried at 50 °C for 12 h to give the final product TIph (2.30 g, 76% yield). Found: N, 5.64%; C, 44.51%; H, 3.52%; on theory: N, 5.79%; C, 44.65%; H, 3.33%.

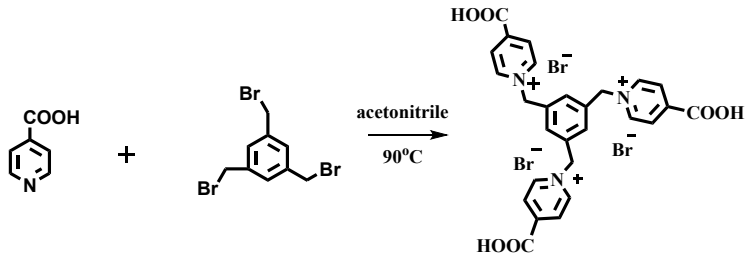

Scheme S4. Synthesis of 1,3,5-tris[(4-carboxypyridino)methyl]-phenyl tribromide (TIph).

2. Synthesis of ionic mesoporous polyamides

Synthesis of DNph-PTA (Scheme S5): A 50 mL flask was charged with DNph (0.286 g, 0.8 mmol) and dichloroethane (DEC, 20 mL), followed by dropwise addition of sulfoxide chloride ($SOCl_2$, 0.2 g, 1.7 mmol). The mixture was stirred at room temperature for 2 h and the suspension became a dark brown solution. Residual $SOCl_2$ was removed by rotary evaporation. The obtained acyl chloride intermediate was dissolved in dry N-methyl pyrrolidone (NMP) (10 mL), followed by dropwise addition of a solution of triethylamine (TEA, 0.1 g, 1 mmol) and bi-phenyl tetramine (PTA, 0.128 g, 0.6 mmol) in 10 mL N,N-dimethylformamide (DMF) at 0 °C. The mixture was heated at 140 °C for

24 h. The precipitate was isolated by filtration, washed with a mixture solution of methanol/water (v/v=1/1), and then dried under vacuum to give a brown powder.

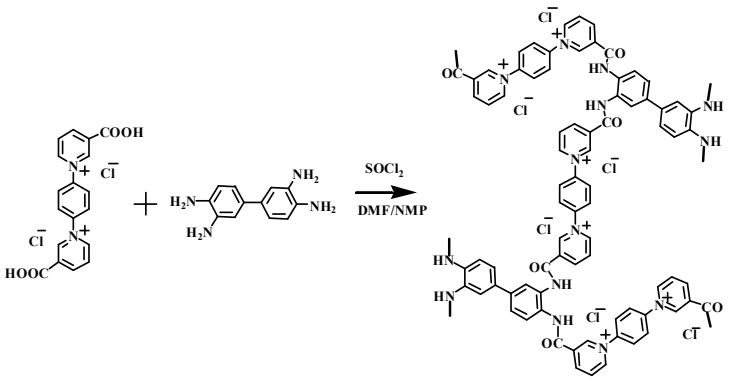

Scheme S5. Synthesis of DNph-PTA.

Synthesis of DNph$_2$-PTA (Scheme S6): A 50 mL flask was charged with DNph$_2$ (0.397 g, 0.8 mmol)and dichloroethane (DEC, 20 mL), followed by dropwise addition of sulfoxide chloride ($SOCl_2$, 0.2 g, 1.7 mmol). The mixture was stirred at room temperature for 2 h and the suspension became a dark brown solution. Residual $SOCl_2$ was removed by rotary evaporation. The obtained acyl chloride intermediate was dissolved in dry N-methyl pyrrolidone (NMP) (10 mL), followed by dropwise addition of a solution of triethylamine (TEA, 0.1g, 1 mmol) and bi-phenyl tetramine (PTA, 0.128 g, 0.6 mmol) in 10 mL N,N-dimethylformamide (DMF) at 0 °C. The mixture was heated at 140 °C for 24 h. The precipitate was isolated by filtration, washed with a mixture solution of methanol/water (v/v=1/1), and then dried under vacuum to give a brown powder.

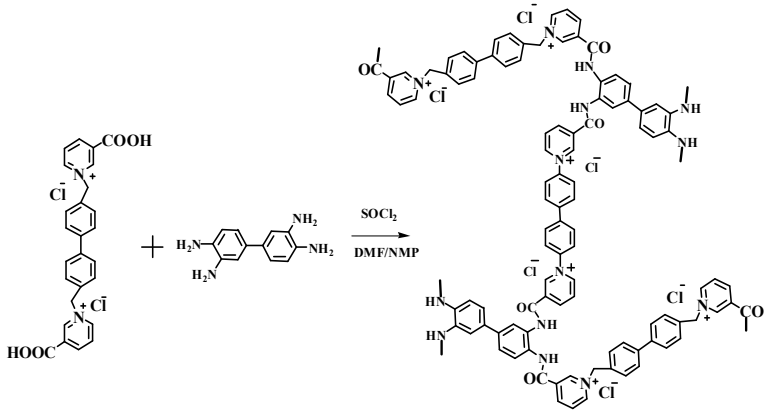

Scheme S6. Synthesis of DNph$_2$-PTA.

Synthesis of TIph-PTA (Scheme S7): A 50 mL flask was charged with TIph (0.581 g, 0.8 mmol) and

dichloroethane (DEC, 20 mL), followed by dropwise addition of sulfoxide chloride ($SOCl_2$, 0.2 g, 1.7 mmol). The mixture was stirred at room temperature for 2 h and the suspension became a dark brown solution. Residual $SOCl_2$ was removed by rotary evaporation. The obtained acyl chloride intermediate was dissolved in dry N-methyl pyrrolidone (NMP) (10 mL), followed by dropwise addition of a solution of triethylamine (TEA, 0.1g, 1 mmol) and bi-phenyl tetramine (PTA, 0.128 g, 0.6 mmol) in 10 mL N,N-dimethylformamide (DMF) at 0 °C. The mixture was heated at 140 °C for 24 h. The precipitate was isolated by filtration, washed with a mixture solution of methanol/water (v/v=1/1), and then dried under vacuum to give a brown powder.

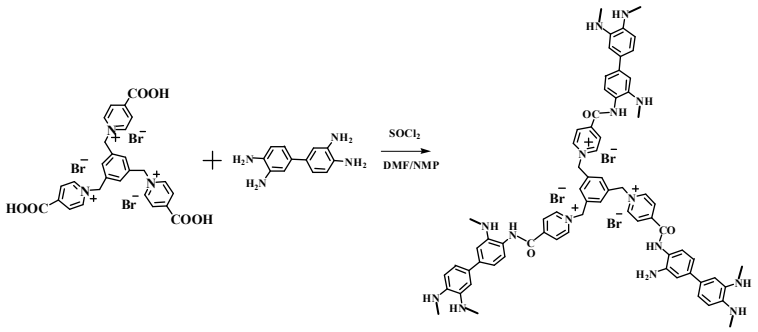

Scheme S7. Synthesis of TIph-PTA.

Synthesis of TNph-PDA (Scheme S8): A 50 mL flask was charged with TNph (0.581 g, 0.8 mmol) and dichloroethane (DEC, 20 mL), followed by dropwise addition of sulfoxide chloride ($SOCl_2$, 0.2 g, 1.7 mmol). The mixture was stirred at room temperature for 2 h and the suspension became a dark brown solution. Residual $SOCl_2$ was removed by rotary evaporation. The obtained acyl chloride intermediate was dissolved in dry N-methyl pyrrolidone (NMP) (10 mL), followed by dropwise addition of a solution of triethylamine (TEA, 0.1g, 1 mmol) and para-phenylene diamine (PDA, 0.130 g, 1.2 mmol) in 10 mL N,N-dimethylformamide (DMF) at 0 °C. The mixture was heated at 140 °C for 24 h. The precipitate was isolated by filtration, washed with a mixture solution of methanol/water (v/v=1/1), and then dried under vacuum to give a brown powder.

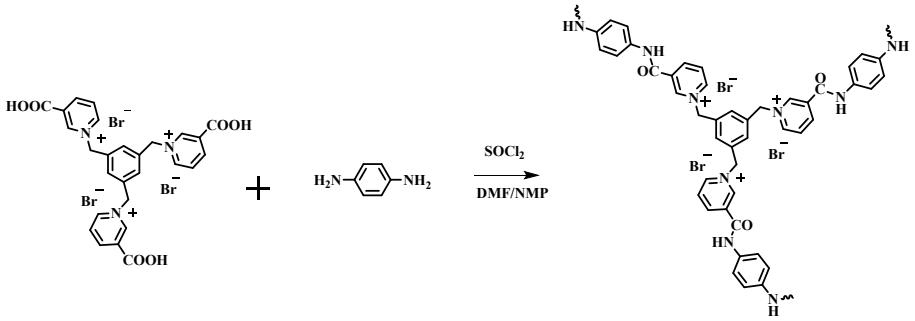

Scheme S8. Synthesis of TNph-PDA.

Synthesis of TNph-TAPB (Scheme S9): A 50 mL flask was charged with TNph (0.581 g, 0.8 mmol) and dichloroethane (DEC, 20 mL), followed by dropwise addition of sulfoxide chloride ($SOCl_2$, 0.2 g, 1.7 mmol). The mixture was stirred at room temperature for 2 h and the suspension became a dark brown solution. Residual $SOCl_2$ was removed by rotary evaporation. The obtained acyl chloride intermediate was dissolved in dry N-methyl pyrrolidone (NMP) (10 mL), followed by dropwise addition of a solution of triethylamine (TEA, 0.1g, 1 mmol) and1,3,5-tris(4-aminophenyl)benzene (TAPB, 0.281 g, 0.8 mmol) in 10 mL N,N-dimethylformamide (DMF) at 0 °C. The mixture was heated at 140 °C for 24 h. The precipitate was isolated by filtration, washed with a mixture solution of methanol/water (v/v=1/1), and then dried under vacuum to give a brown powder.

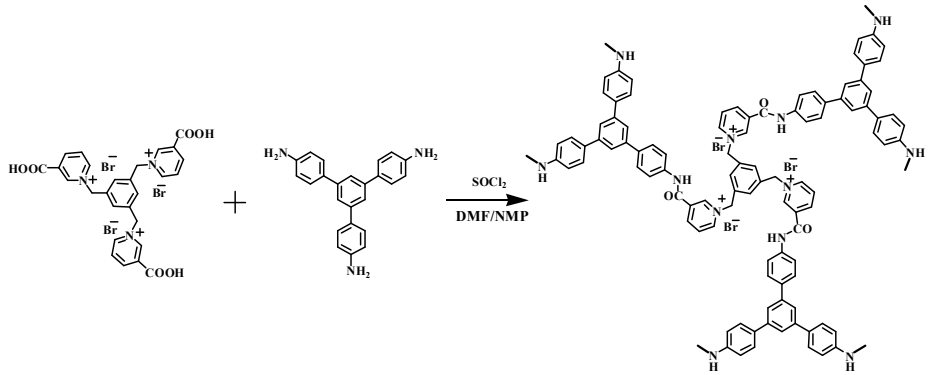

Scheme S9. Synthesis of TNph-TAPB.

Synthesis of TNph-TAPM (Scheme S10): A 50 mL flask was charged with TNph (0.581 g, 0.8 mmol) and dichloroethane (DEC, 20 mL), followed by dropwise addition of sulfoxide chloride ($SOCl_2$, 0.2 g, 1.7 mmol). The mixture was stirred at room temperature for 2 h and the suspension became a dark brown solution. Residual $SOCl_2$ was removed by rotary evaporation. The obtained acyl chloride intermediate was dissolved in dry N-methyl pyrrolidone (NMP) (10 mL), followed by dropwise addition of a solution of triethylamine (TEA, 0.1 g, 1 mmol) andtetra(4-aminophenyl)methane (TAPM, 0.228 g, 0.6 mmol) in 10 mL N,N-dimethylformamide (DMF) at 0 °C. The mixture was heated at 140 °C for 24 h. The precipitate was isolated by filtration, washed with a mixture solution of methanol/water (v/v=1/1), and then dried under vacuum to give a brown powder.

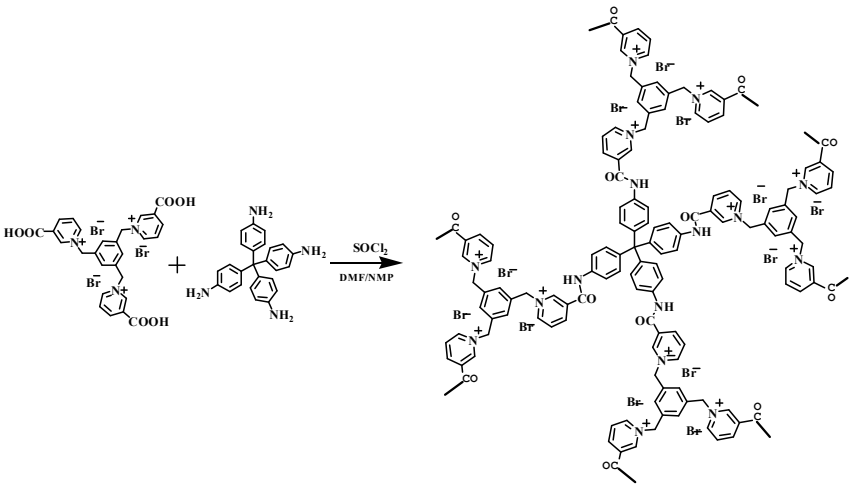

Scheme S10. Synthesis of TNph-TAPM.

Synthesis of TA-PTA (Scheme S11): A 50 mL flask was charged with trimesic acid (TA, 0.168 g, 0.8 mmol)and dichloroethane (DEC, 20 mL), followed by dropwise addition of sulfoxide chloride ($SOCl_2$, 0.2 g, 1.7 mmol). The mixture was stirred at room temperature for 2 h and the suspension became a dark brown solution. Residual $SOCl_2$ was removed by rotary evaporation. The obtained acyl chloride intermediate was dissolved in dry N-methyl pyrrolidone (NMP) (10 mL), followed by dropwise addition of a solution of triethylamine (TEA, 0.1g, 1 mmol) andbi-phenyl tetramine (PTA, 0.128 g, 0.6 mmol) in 10 mL N,N-dimethylformamide (DMF) at 0 °C. The mixture was heated at 140 °C for 24 h. The precipitate was isolated by filtration, washed with a mixture solution of methanol/water (v/v=1/1), and then dried under vacuum to give a brown powder.

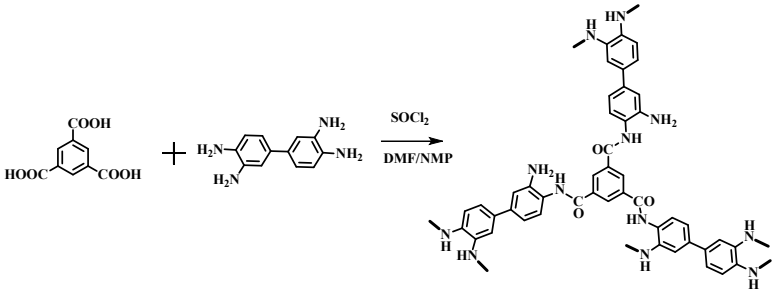

Scheme S11. Synthesis of TA-PTA.

Synthesis of PDMBr (Scheme S12): 1-Vinylimidazole (5.00 g, 53.2 mmol) and CH_2Br_2 (4.62 g, 26.6 mmol) were dissolved in 5 mL THF. After stirring at room temperature for 1 h, the mixture was solvothermally treated at 100 °C for 24 h. After cooling to room temperature, the obtained crude salt was washed with diethyl ether and dried under vacuum, giving the light yellow powder product, 3,3-methylene-divinylimidazole dibromide ([C1DVIM]Br). [C1DVIM]Br (0.3 g), [C4MIM]Br (6 g), H_2O

(0.75 mL) and AIBN (0.03 g) were placed in a Teflon-lined stainless steel autoclave. Subsequently, the above mixture was stirred for 2 h to give a homogeneous and transparent solution. The polymerization was triggered by statically heating at 100 °C for 24 h. The solidified composite was washed with water and then dried under vacuum at 80 °C.

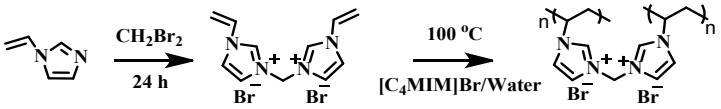

Scheme S12. Synthesis of PDMBr.

Supplementary Fig.s

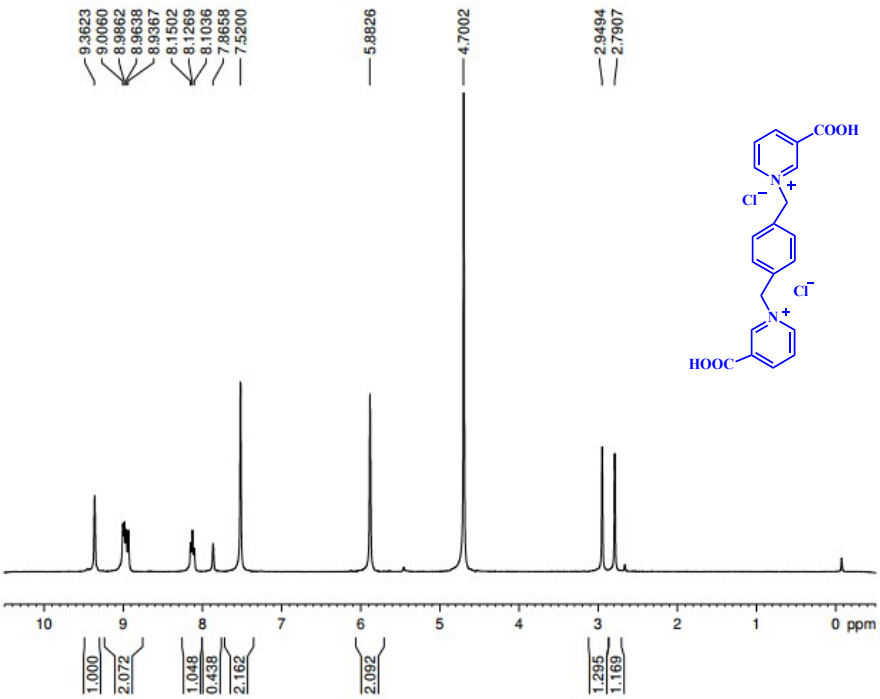

Fig. S1 ^{1}H NMR spectrum of DNph.

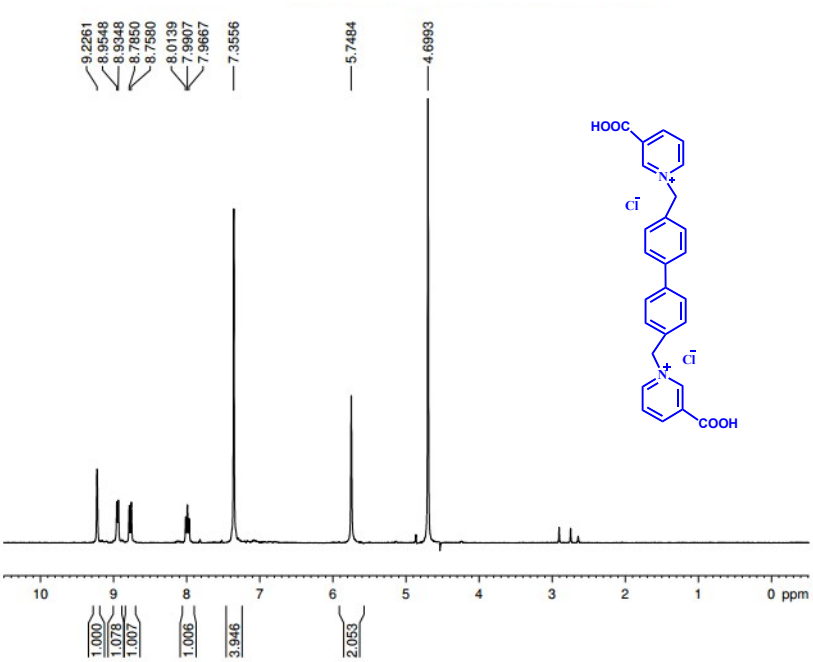

Fig. S2 ^{1}H NMR spectrum of $DNph_2$.

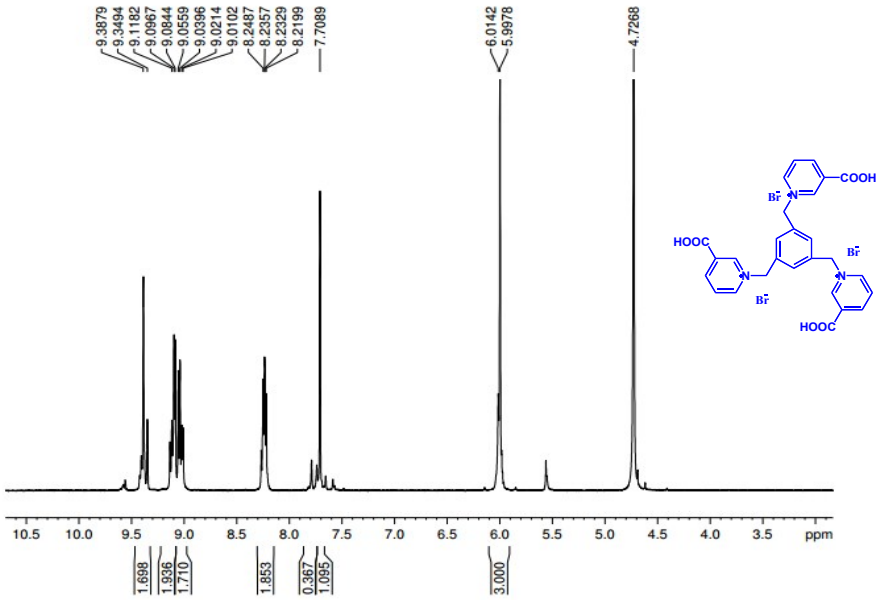

Fig. S3 ^{1}H NMR spectrum of TNph.

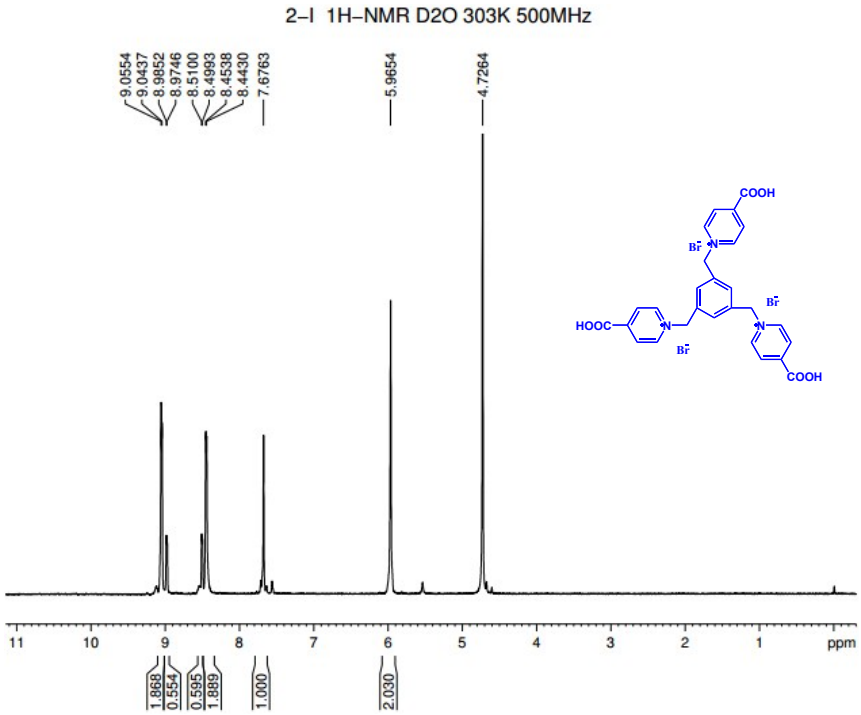

Fig. S4 ^{1}H NMR spectrum of TIph.

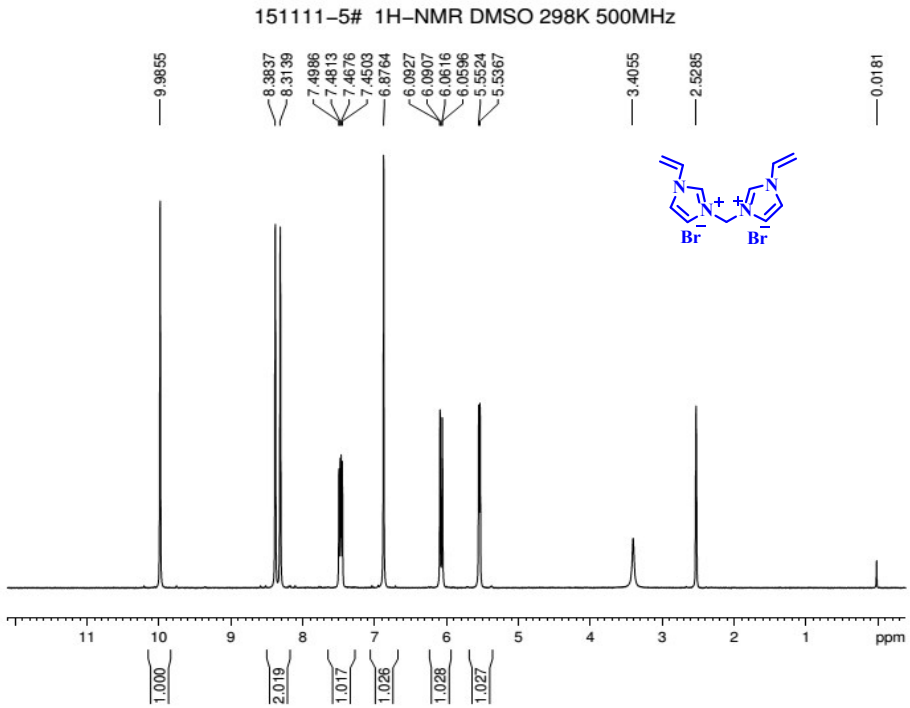

Fig. S5 ^{1}H NMR spectrum of [C_1DVIM]Br.

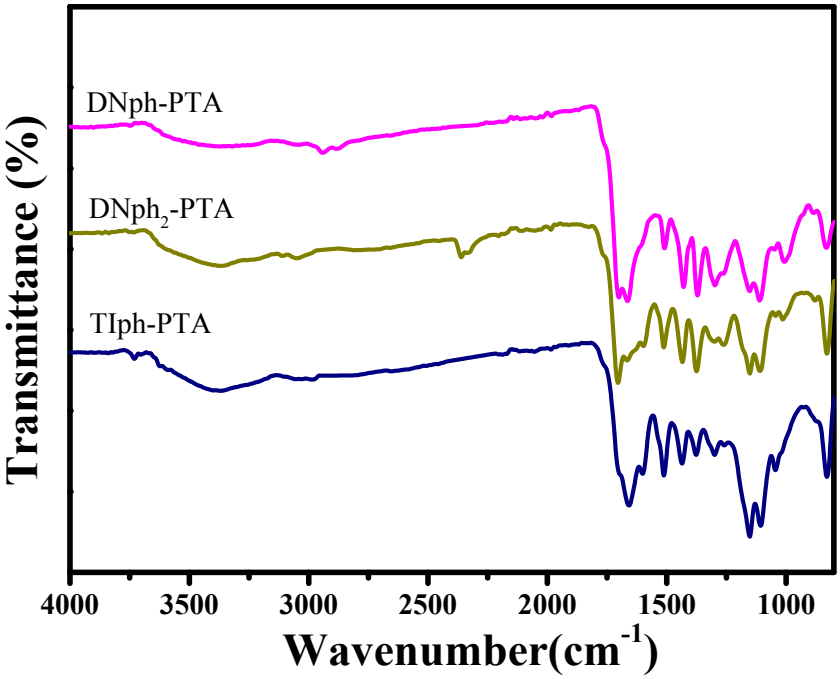

Fig. S6 FTIR spectra of DNph-PTA, $DNph_2$-PTA and TIph-PTA.

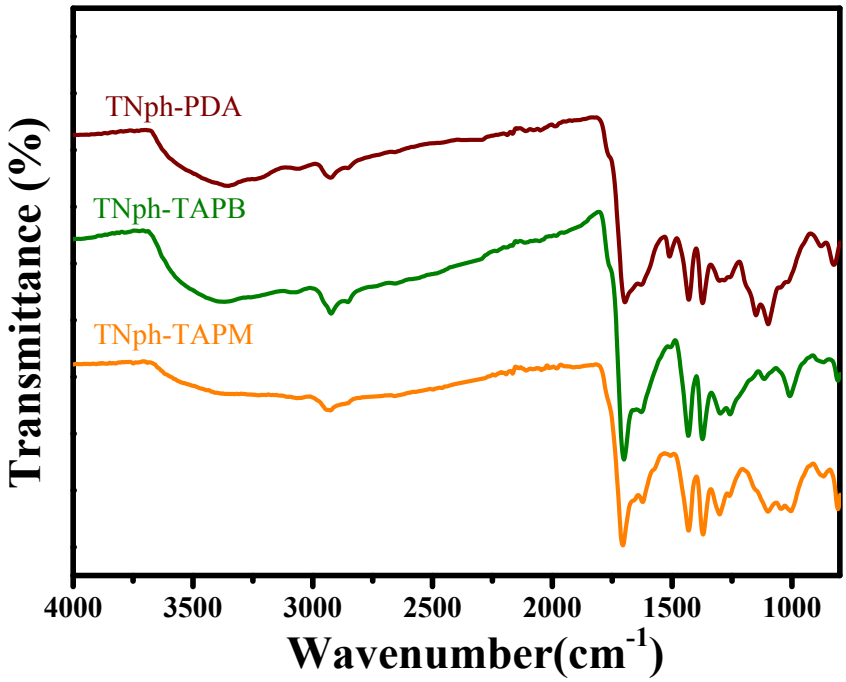

Fig. S7 FTIR spectra of TNph-PDA, TNph-TAPB and TNph-TAPM.

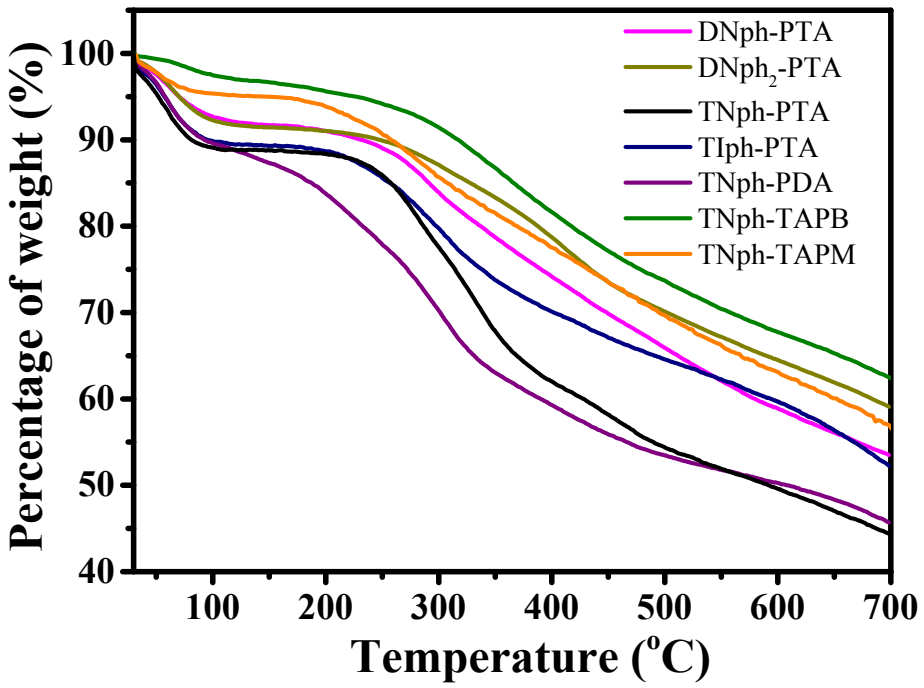

Fig. S8 TG curves of DNph-PTA, DNph$_2$-PTA, TNph-PTA, TIph-PTA, TNph-PDA, TNph-TAPB, and TNph-TAPM.

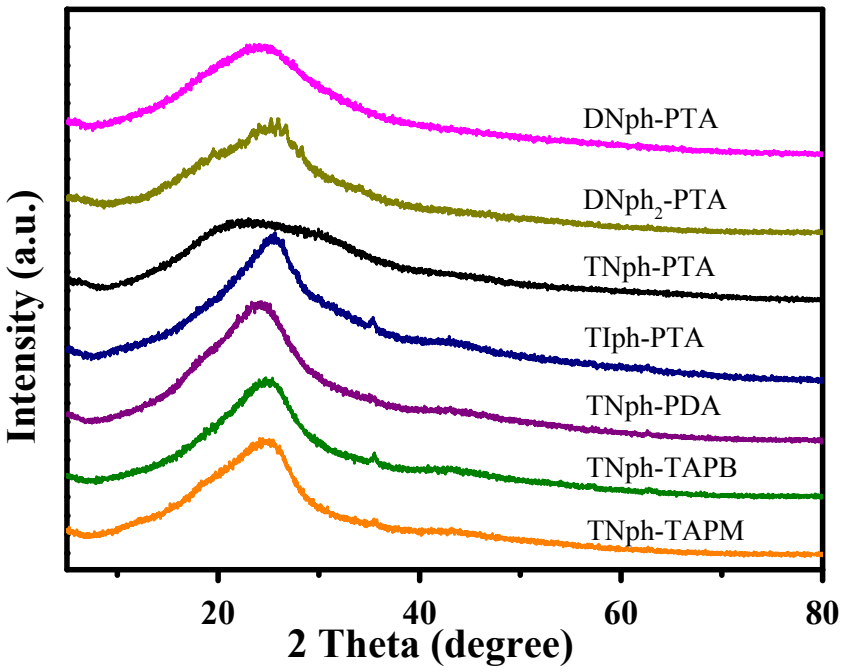

Fig. S9 XRD patterns of DNph-PTA, DNph$_2$-PTA, TNph-PTA, TIph-PTA, TNph-PDA, TNph-TAPB, and TNph-TAPM.

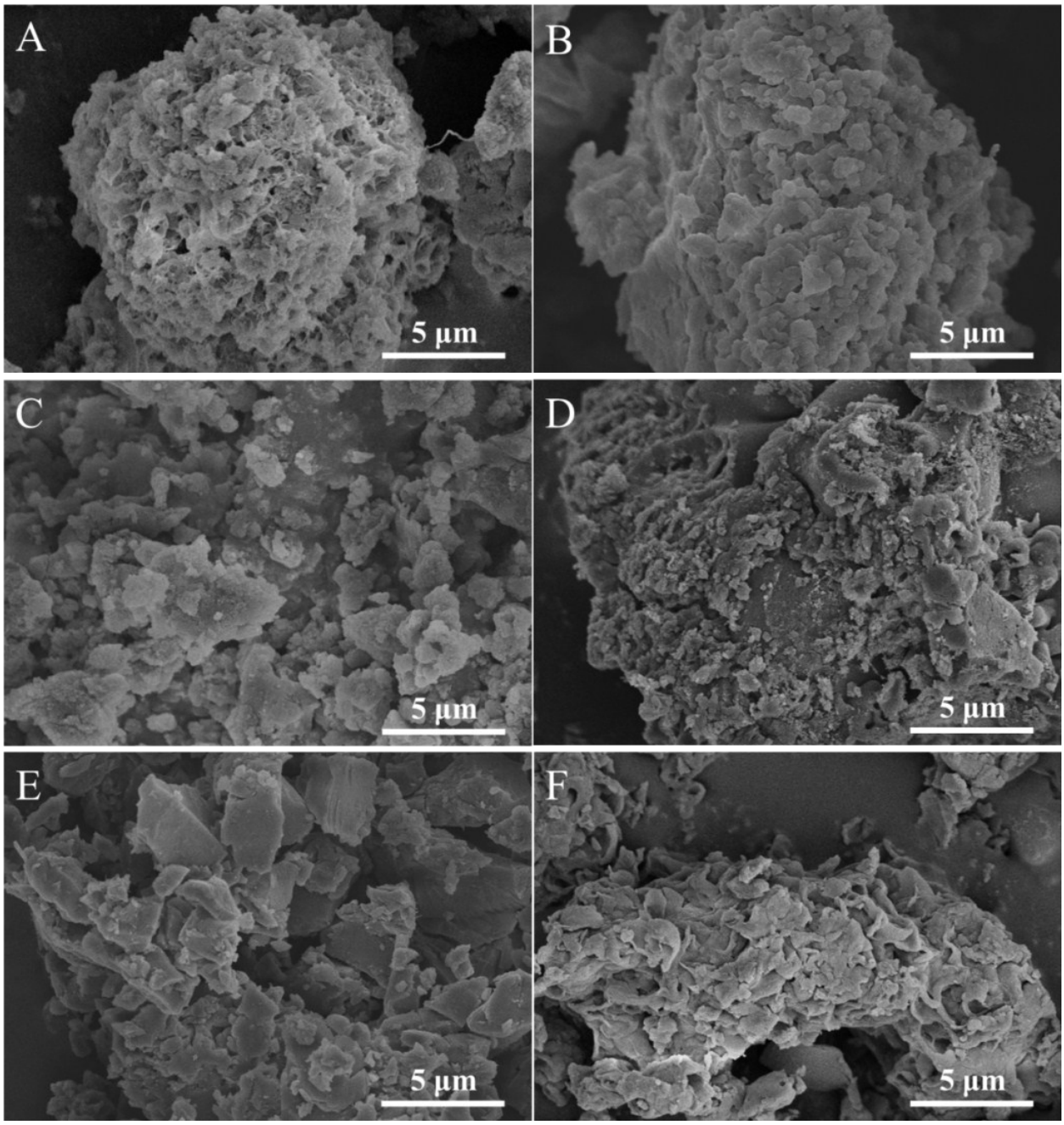

Fig. S10 SEM images of (A) DNph-PTA, (B) $DNph_2$-PTA, (C) TIph-PTA, (D) TNph-PDA, (E) TNph-TAPB, and (F) TNph-TAPM.

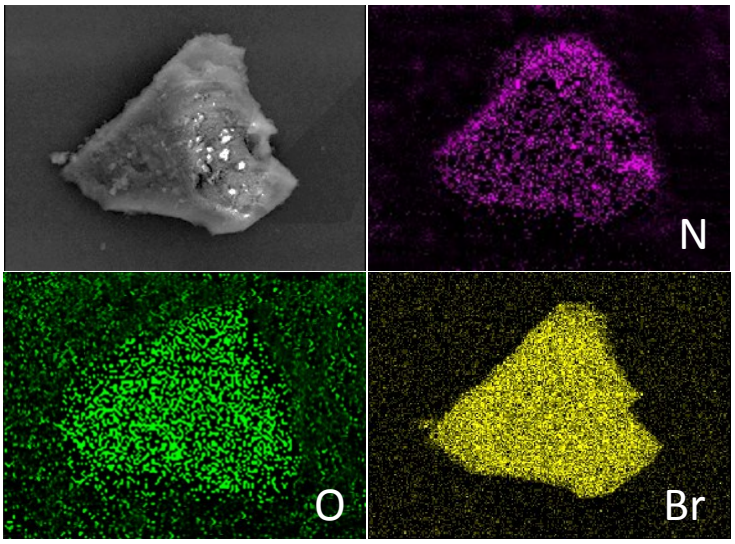

Fig. S11 SEMand elemental mapping images of N, O and Br for TNph-PTA.

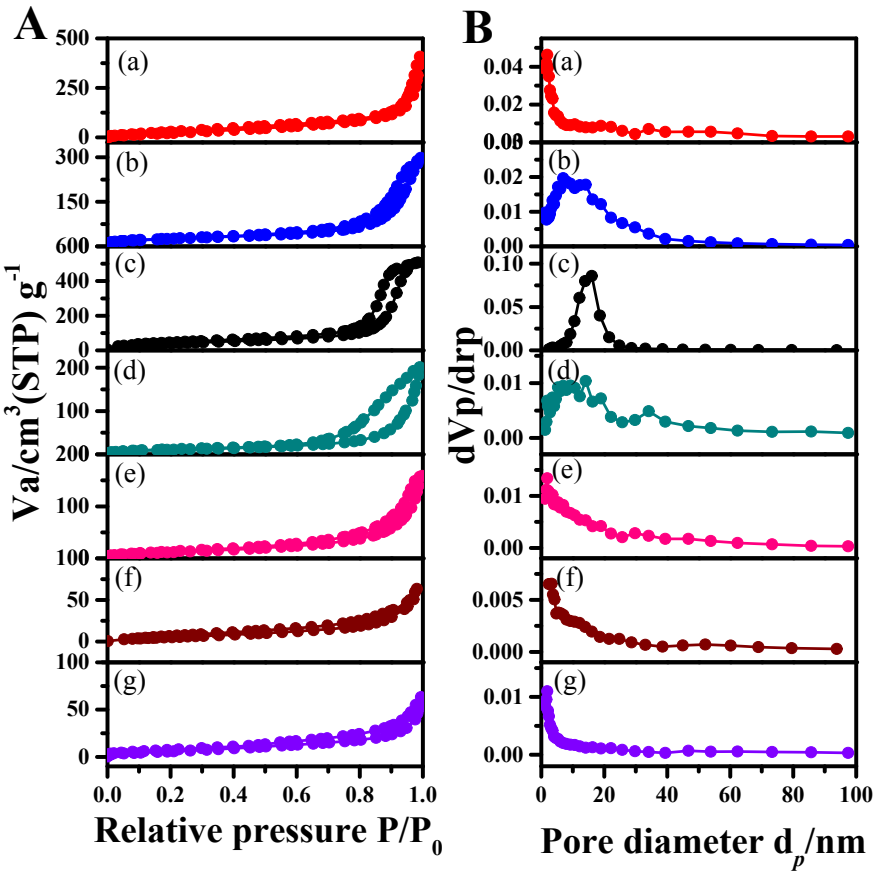

Fig. S12 (A) N_2 sorption isotherms and (B) pore size distribution curves of iMPAs. The synthetic procedure was same as TNph-PTA except by using solvents of (a) NMP (15 mL), (b) DMF (15 mL), (c) DMF/NMP (10 mL/10 mL), (d) DMF/NMP (5 mL/10 mL), (e) DMF/NMP (10 mL/5 mL), (f) THF/NMP (10 mL/10 mL), (g) TMB/NMP (10 mL/10 mL). Synthesis condition: TNph 0.8 mmol, PTA 0.6 mmol, $SOCl_2$ 1.7 mmol, TEA 1 mmol, 140 ^{o}C, 24 h.

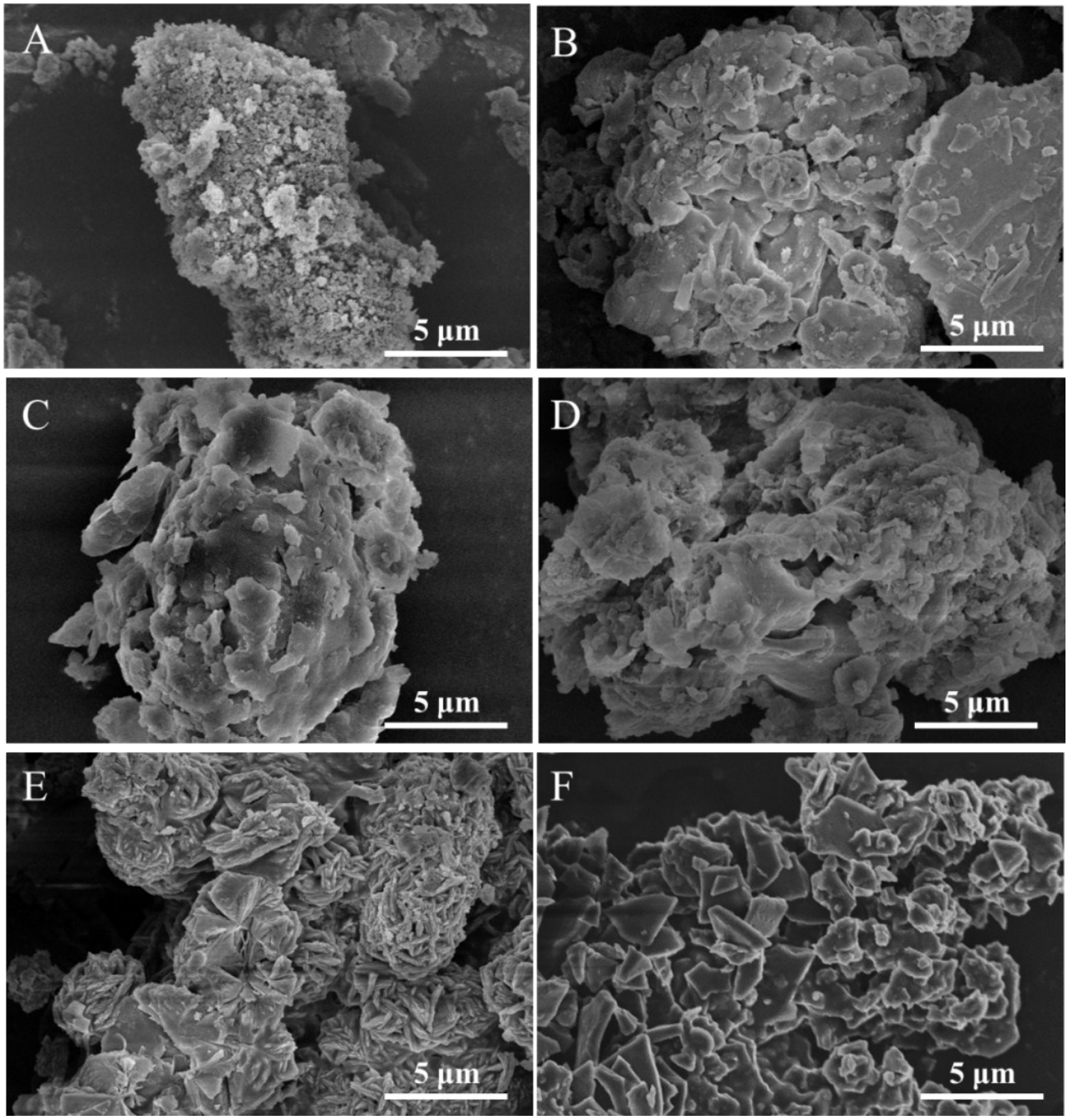

Fig. S13 SEM images of iMPAs. The synthetic procedure was same as that of TNph-PTA except by using solvents of (A) NMP 15 mL, (B) DMF 15 mL, (C) DMF/NMP (5 mL/10 mL), (D) DMF/NMP (10 mL/5 mL), (E) THF/NMP (10 mL/10 mL), and (F) TMB/NMP (10 mL/10 mL), respectively.

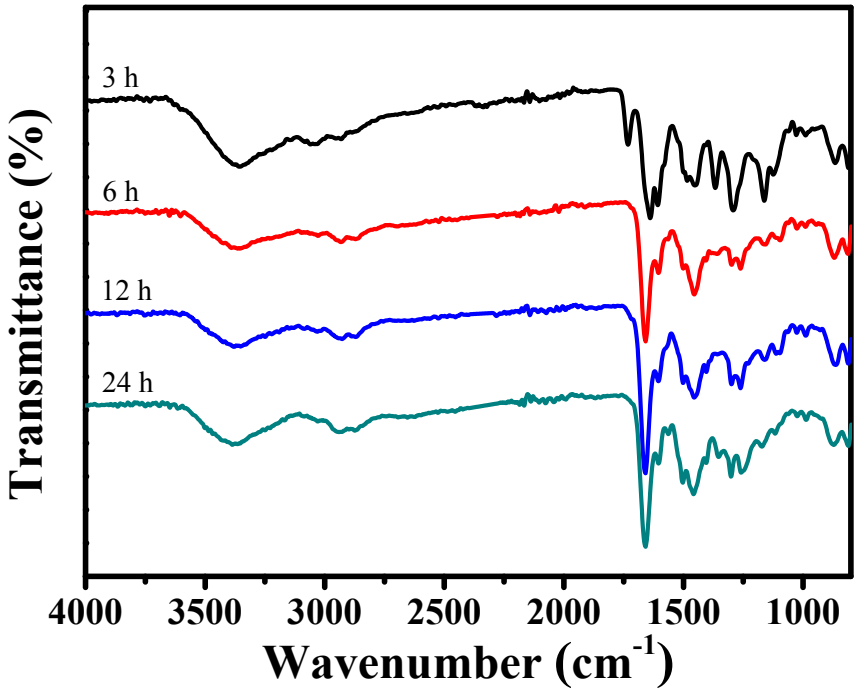

Fig. S14 FTIR spectra of iMPAs. The synthetic procedure was same as TNph-PTA except for polymerization time of 3, 6, 12, and 24 h, respectively.

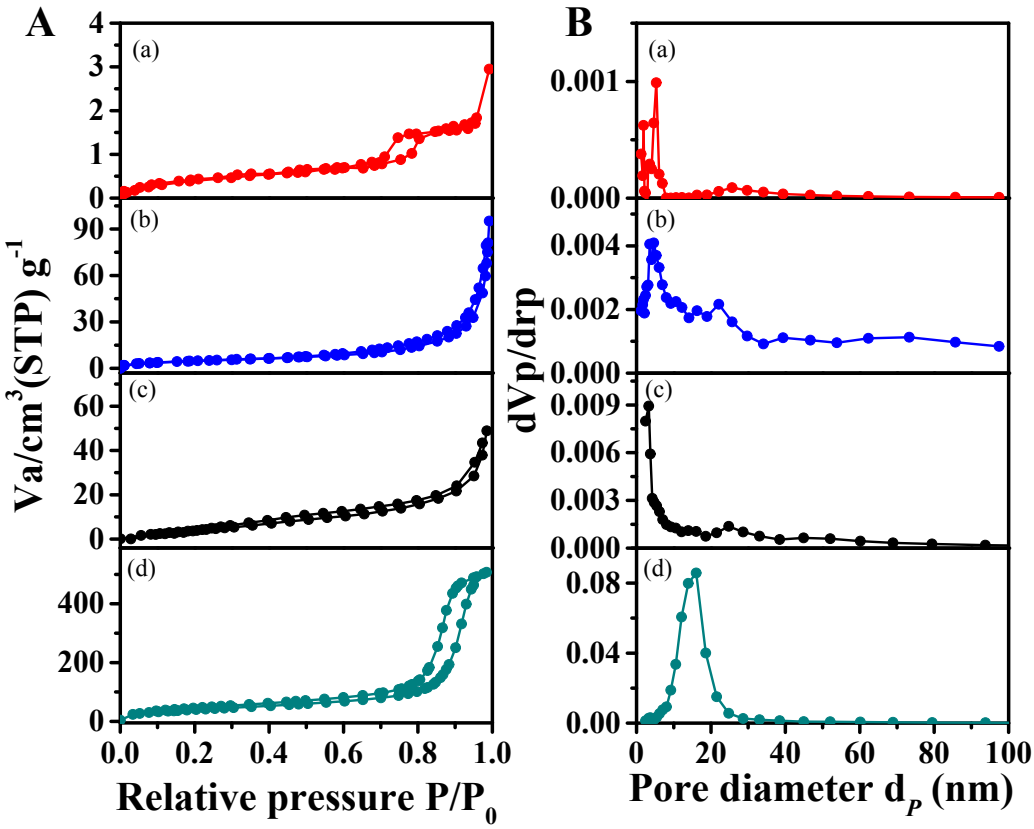

Fig. S15 (A) N_2 sorption isotherms and (B) pore size distribution curves of iMPAs. The synthetic procedure was same as TNph-PTA except for polymerization time of(a) 3 h, (b) 6 h, (c) 12 h, and (d) 24 h, respectively.

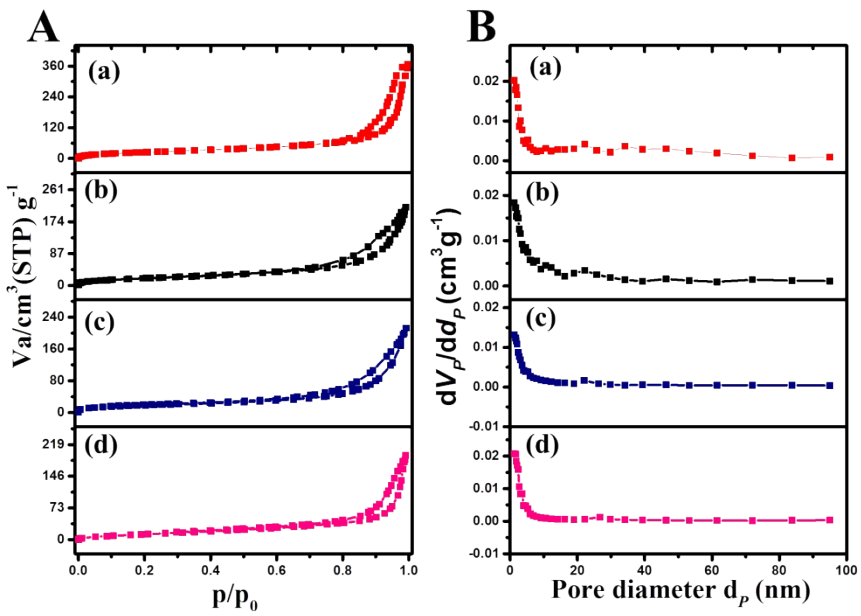

Fig. S16 (A) N_2 sorption isotherms and (B) pore size distribution curves of (a) $Ru_{0.5}$@TNph-PTA, (b) $Ru_{1.5}$@TNph-PTA, (c) Ru_5@TNph-PTA and (d) Ru_8@TNph-PTA.

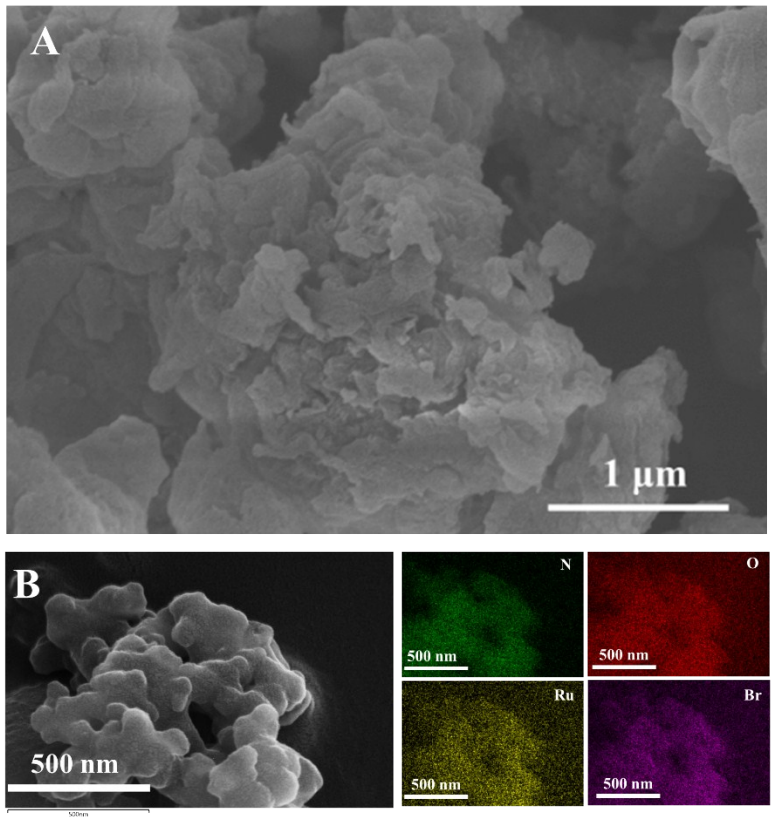

Fig. S17 (A) SEM and (B) SEM mapping images of $Ru_{1.5}$@TNph-PTA.

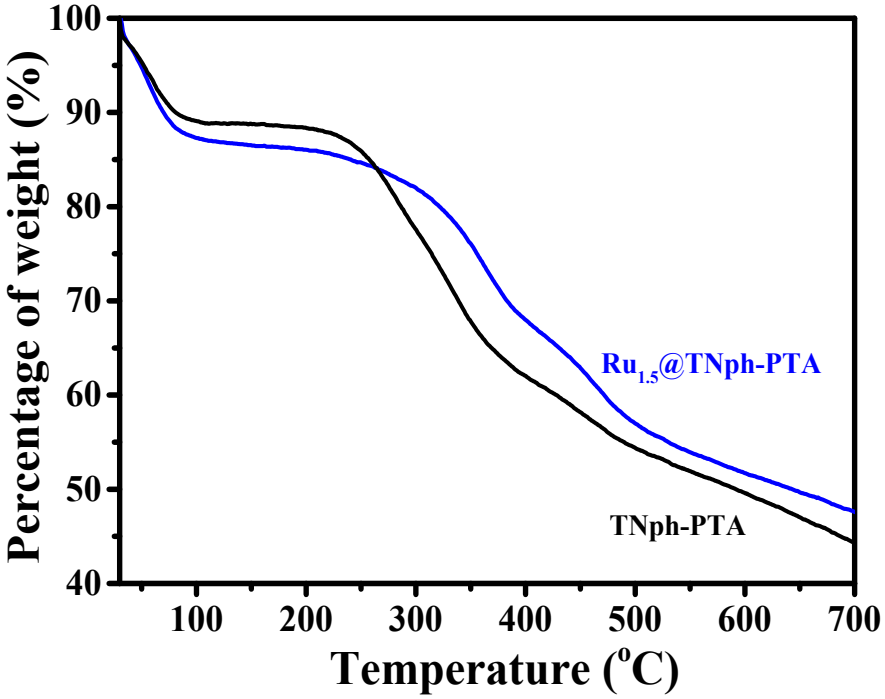

Fig. S18 TG curves of TNph-PTA and $Ru_{1.5}$@TNph-PTA.

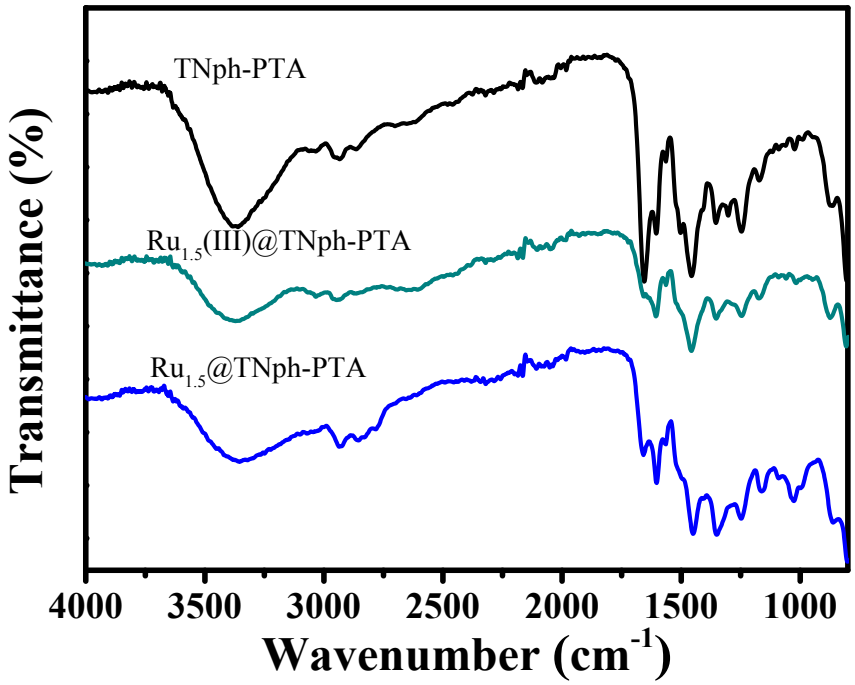

Fig. S19 FTIR spectra of TNph-PTA, $Ru_{1.5}$(III)@TNph-PTA and $Ru_{1.5}$@TNph-PTA.

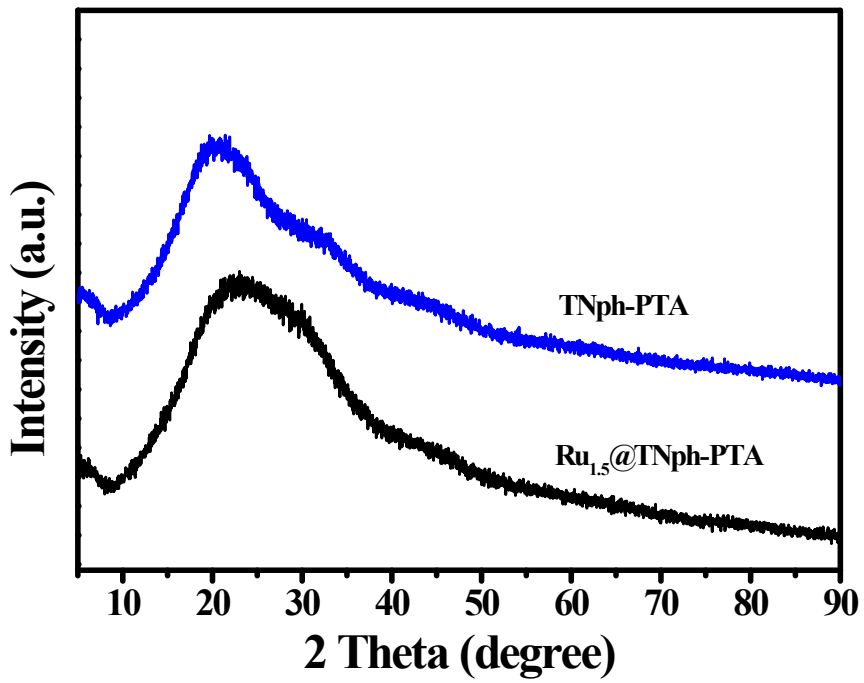

Fig. S20 XRD patterns of TNph-PTA and $Ru_{1.5}$@TNph-PTA.

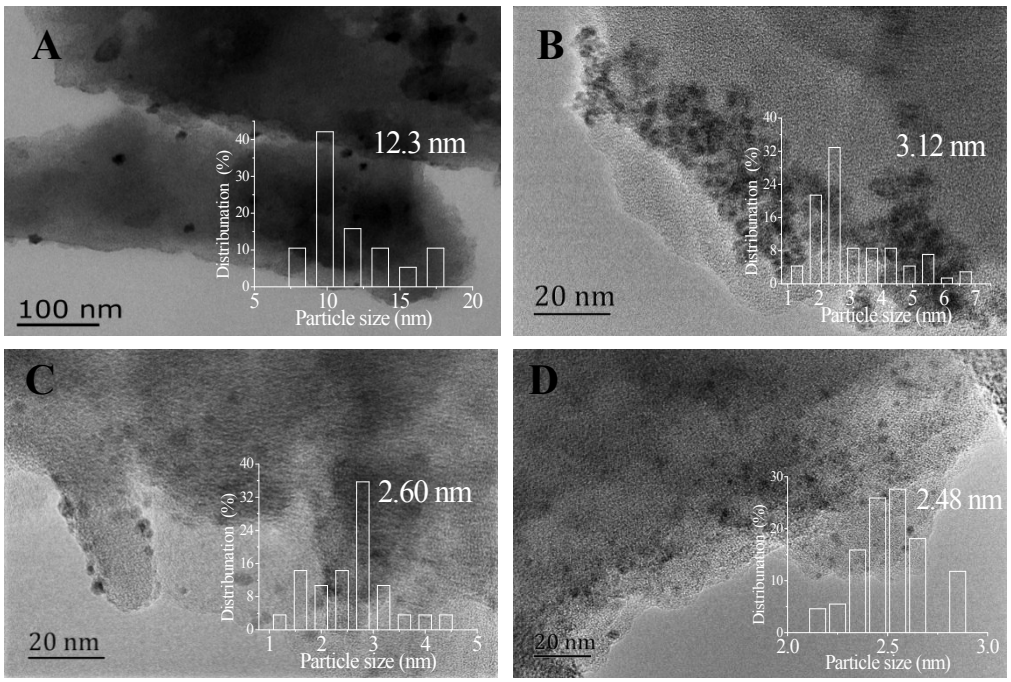

Fig. S21 TEM images of (A) Ru/C, (B) $Ru_{1.5}$@TNph-PTA-N, (C) $Ru_{1.5}$@TA-PTA, and (D) $Ru_{1.5}$@PDMBr.

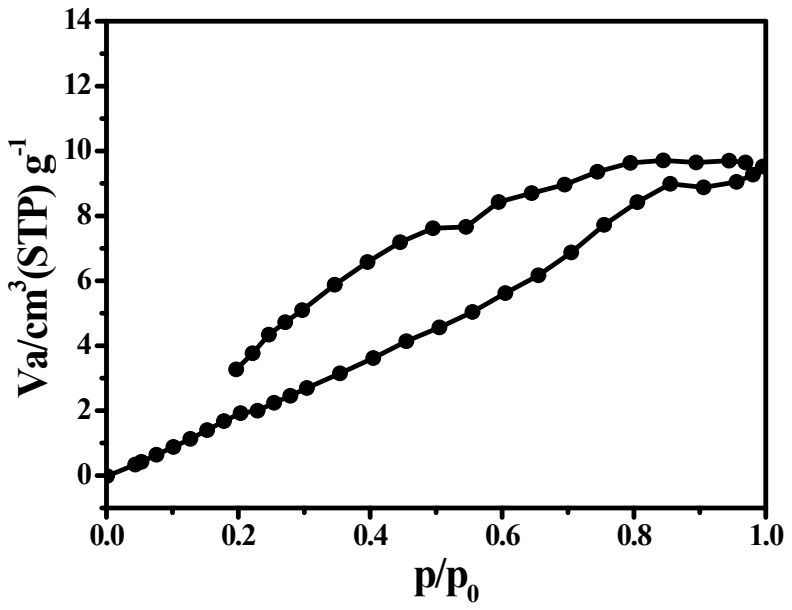

Fig. S22 N_2 sorption isotherm of TNph-PTA-N.

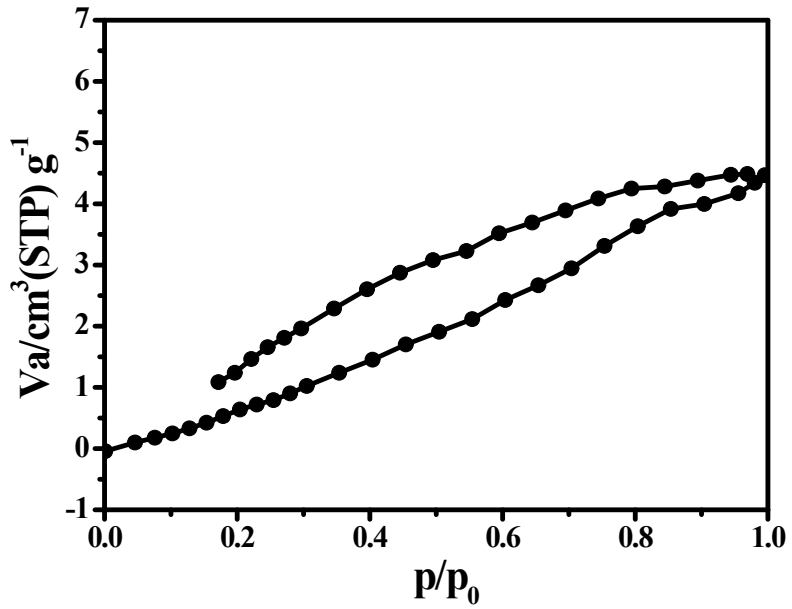

Fig. S23 N_2 sorption isotherm of $Ru_{1.5}$@TNph-PTA-N.

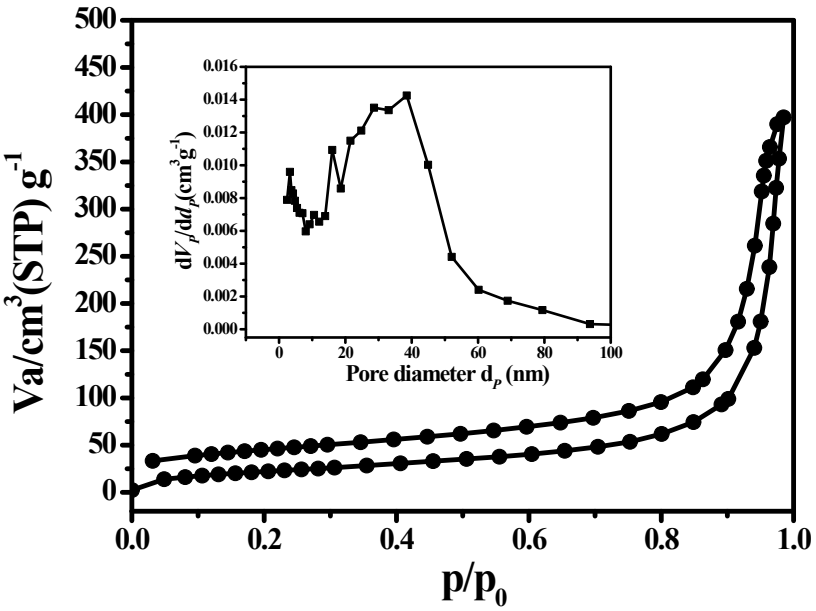

Fig. S24 N_2 sorption isotherms (inset: pore size distribution curves) of TA-PTA.

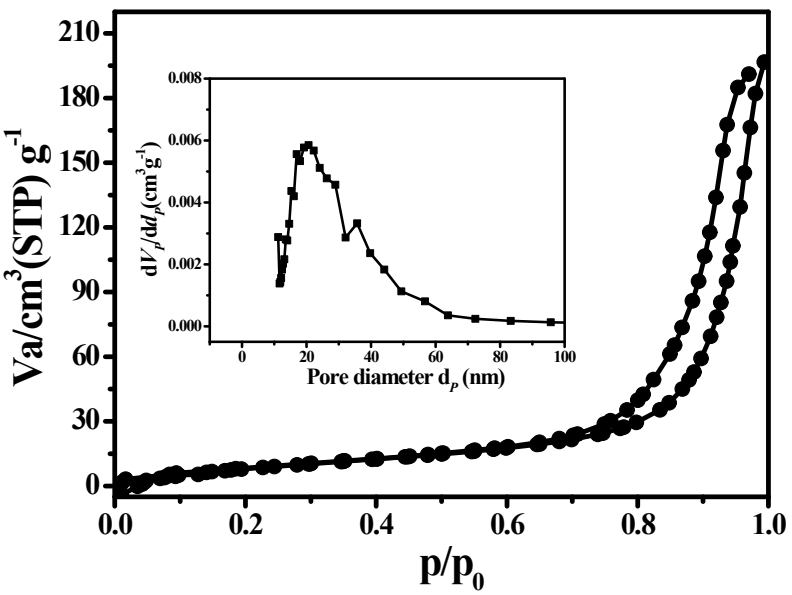

Fig. S25 N_2 sorption isotherm (inset: pore size distribution curve) of $Ru_{1.5}$@TA-PTA.

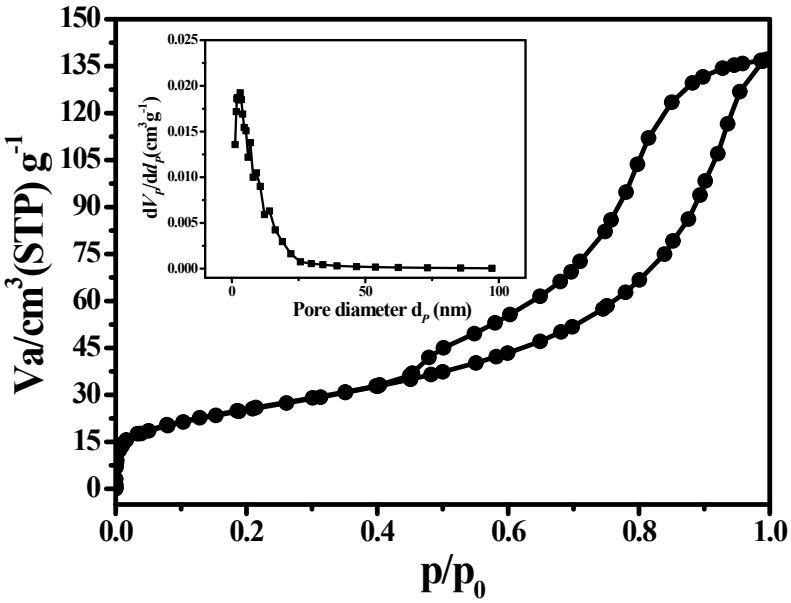

Fig. S26 N_2 sorption isotherm (inset: pore size distribution curve) of PDMBr.

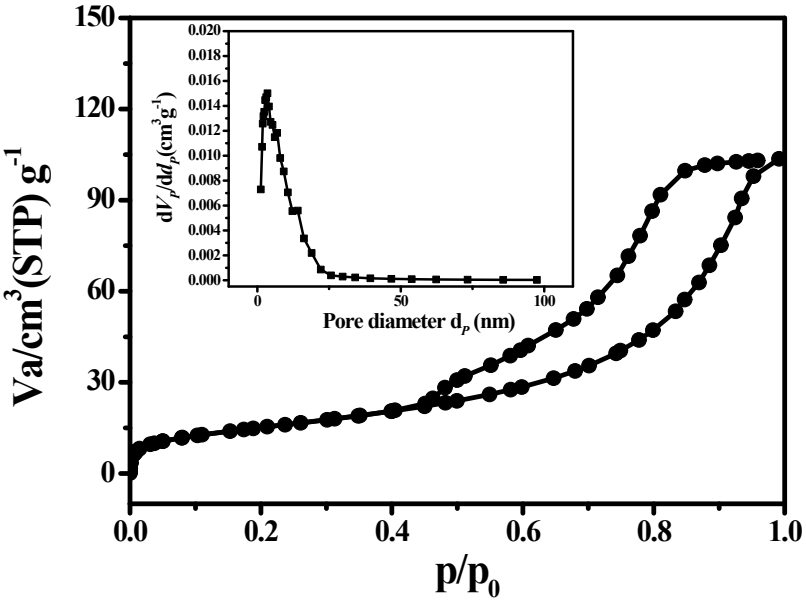

Fig. S27 N_2 sorption isotherm (inset: pore size distribution curve) of $Ru_{1.5}$@PDMBr.

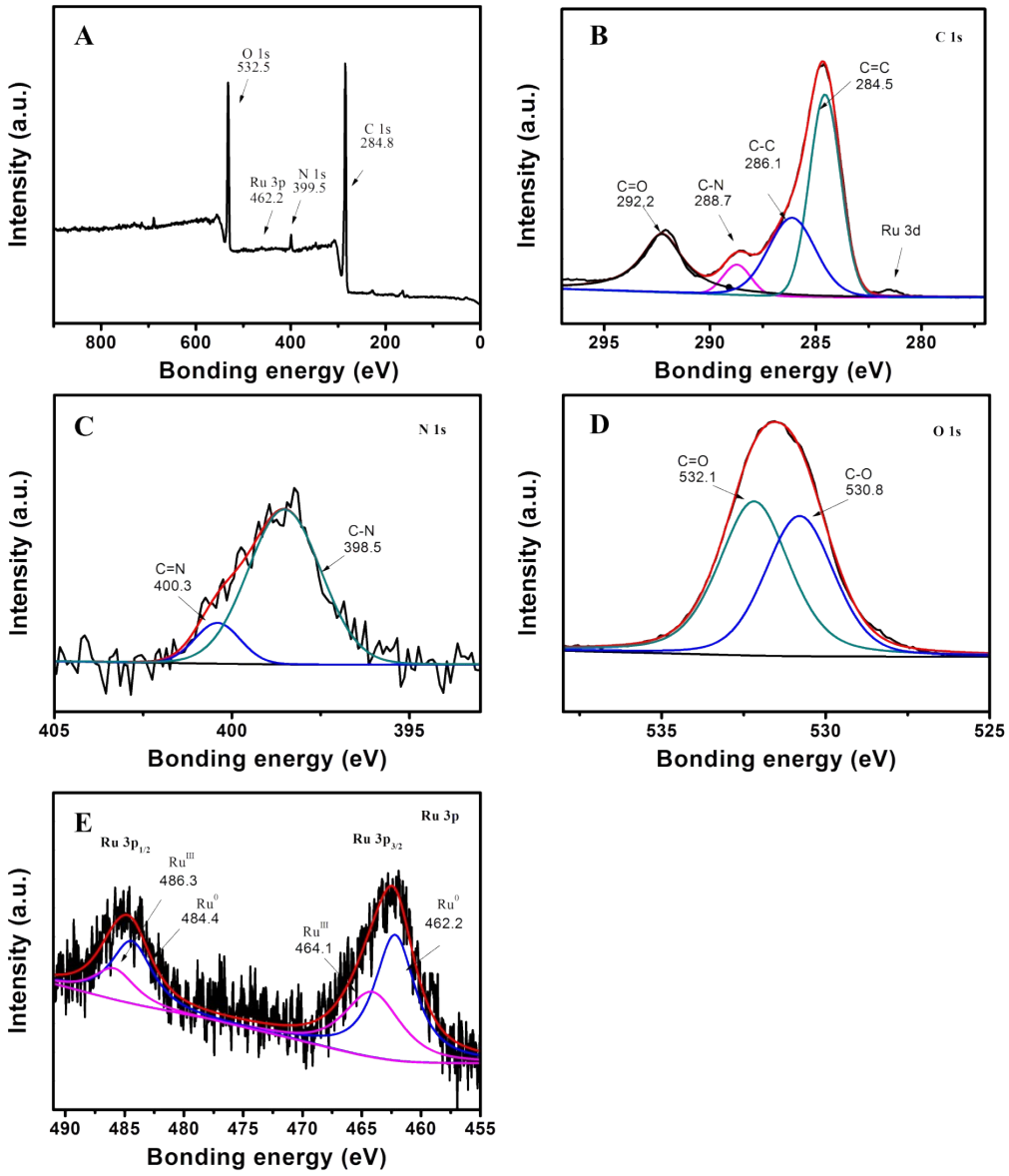

Fig. S28 (A) survey scan, (B) C 1s, (C) N 1s, (D) O 1s, and (E) Ru 3p XPS spectra of $Ru_{1.5}$@TA-PTA.

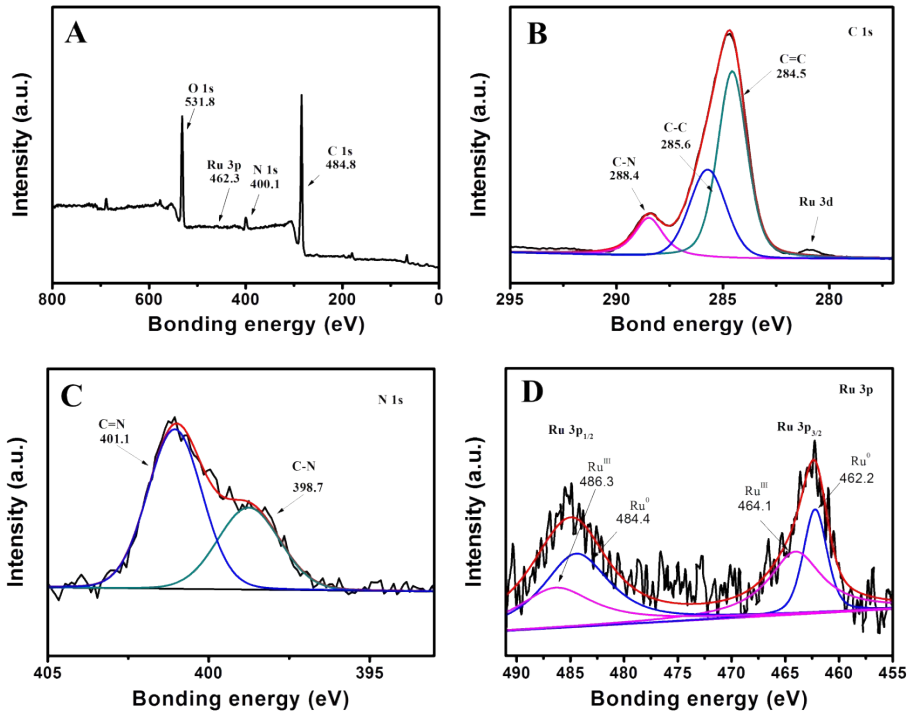

Fig. S29 (A) survey scan, (B) C 1s, (C) N 1s, (D) Ru 3p XPS spectra of $Ru_{1.5}$@PDMBr.

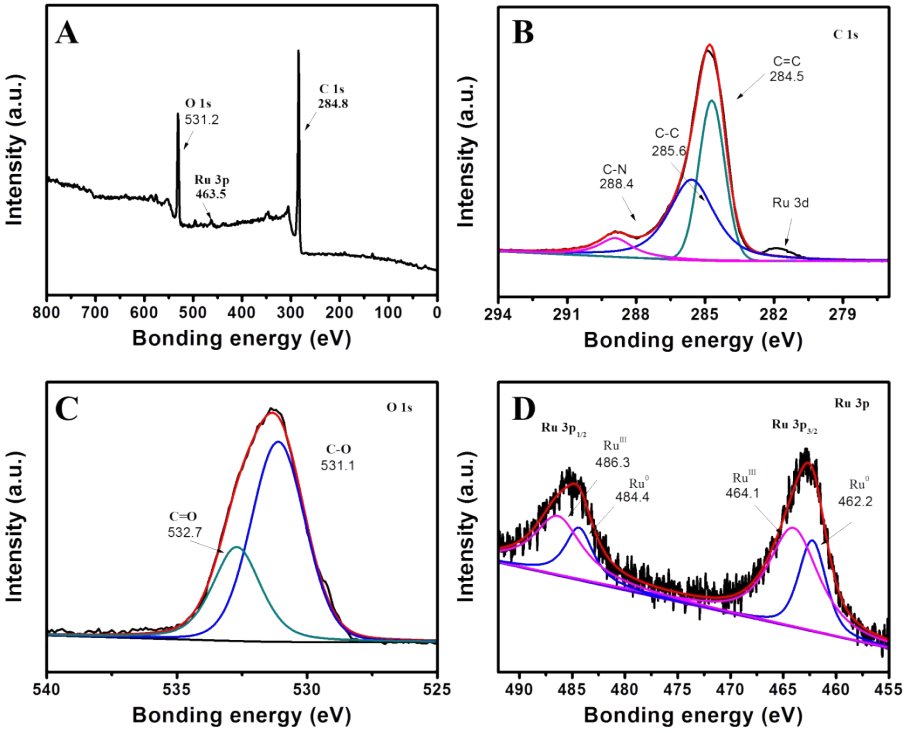

Fig. S30 (A) survey scan, (B) C 1s, (C) N 1s, (D) O 1s, and (E) Ru 3p XPS spectra of Ru/C.

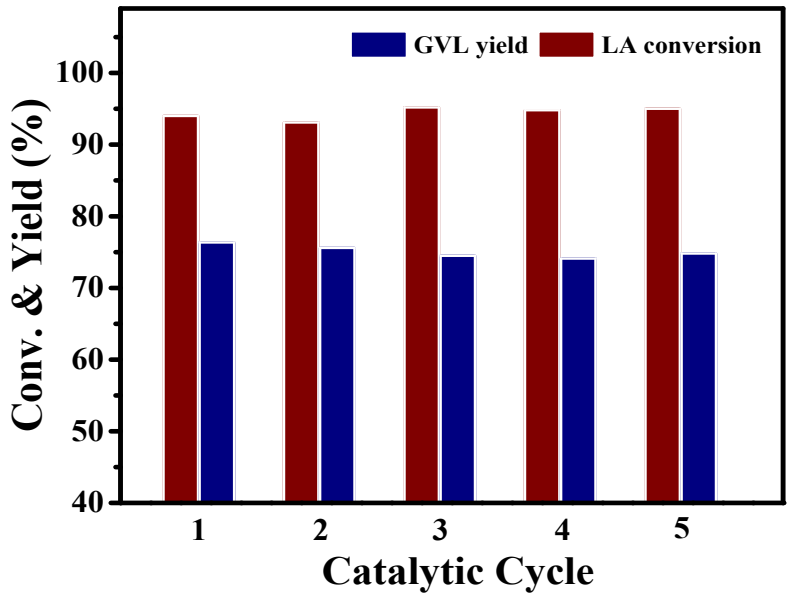

Fig. S31 Recyclability of $Ru_{1.5}$@TNph-PTA for hydrogenation of LA to GVL. Reaction conditions: 1 mmol LA, 4 mL water, LA/Ru=350, 70 °C, 4 h, 1 MPa.

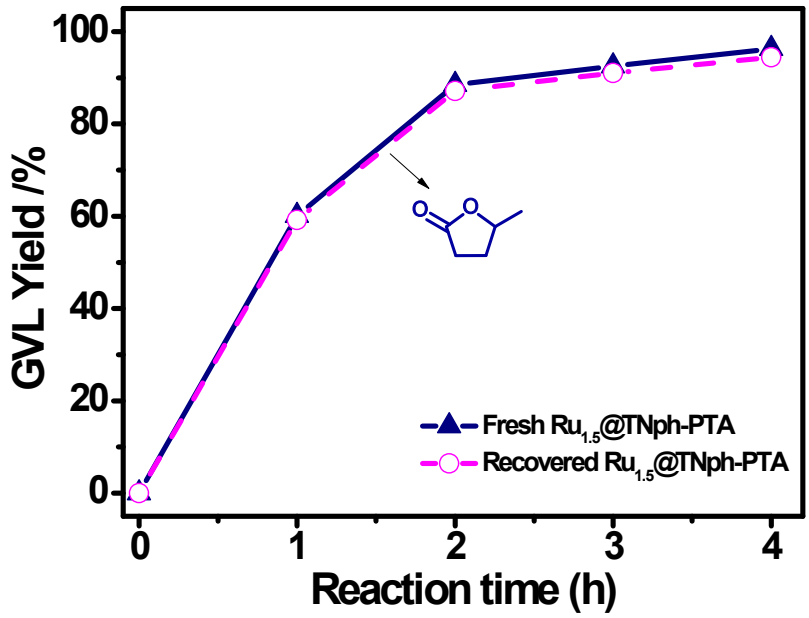

Fig. S32 Kinetic curves of the fresh catalyst (solid lines) and recovered catalyst (dashed line, the 5th run). Reaction conditions: 1 mmol LA, 4 mL water, LA/Ru=350, 4 h, 1 MPa 150 °C.

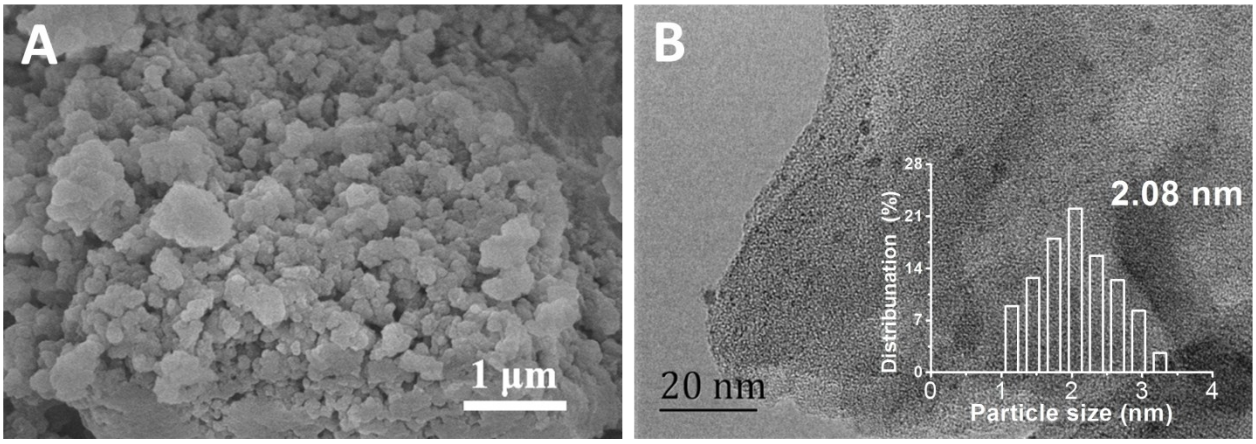

Fig. S33 (A) SEM and (B) TEM image of recovered $Ru_{1.5}$@TNph-PTA.

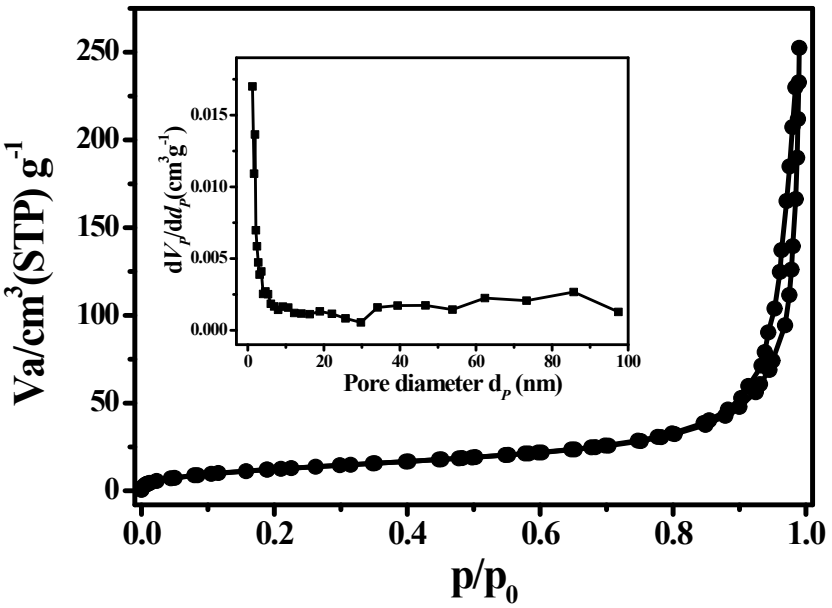

Fig. S34 N_2 sorption isotherm (inset: pore size distribution curve) of recovered $Ru_{1.5}$@TNph-PTA.

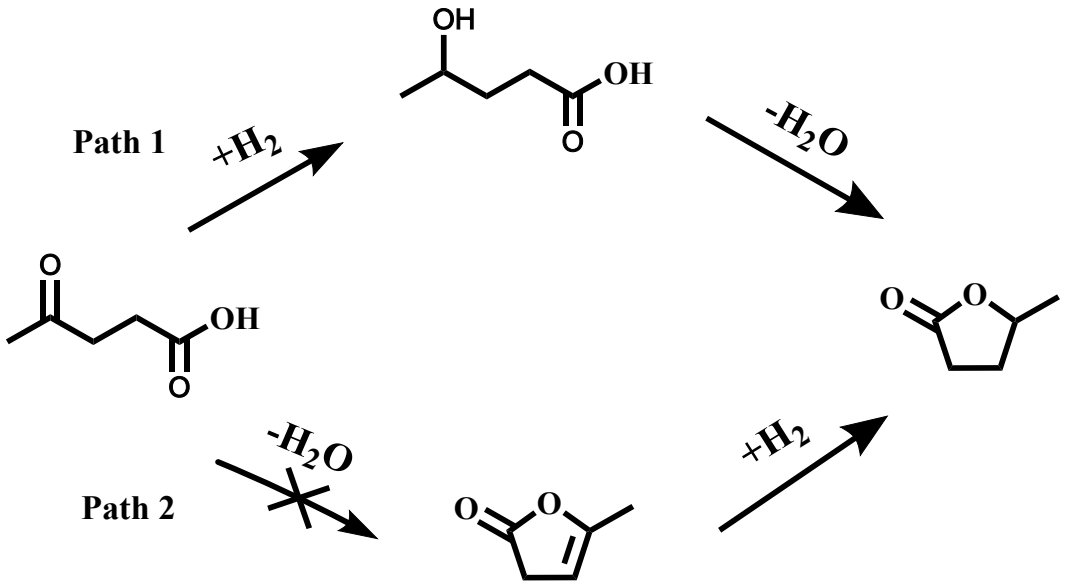

Fig. S35 Hydrogenation and dehydration of LA to produce GVL. In this system Path 1 was occurred.

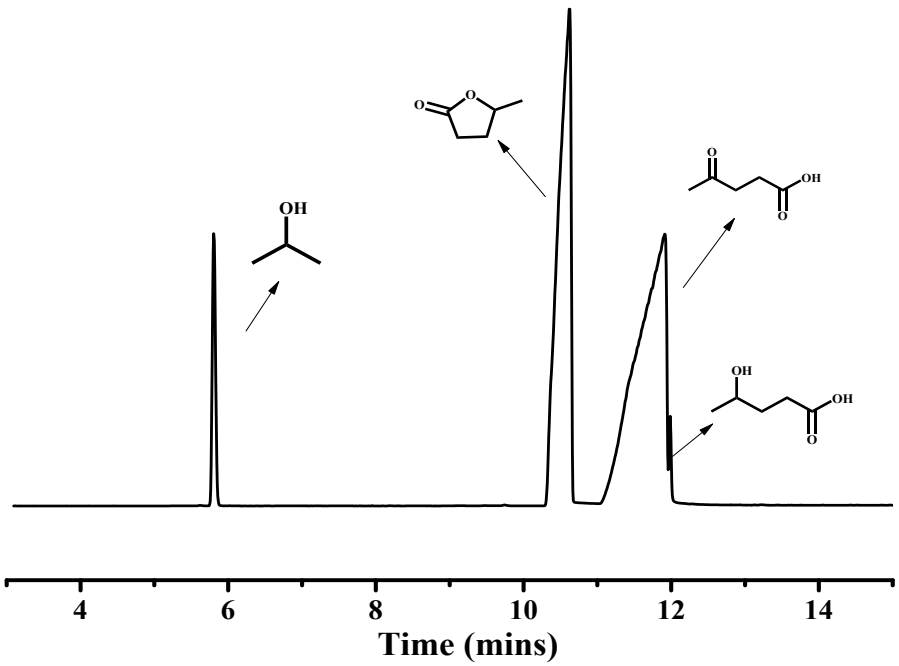

Fig. S36 GC-MS analysis of the liquid phase after reaction. Reaction conditions: catalyst $Ru_{1.5}$@TNph-PTA 19 mg, LA 10 mmol, water 4 mL, LA/Ru=3500, 150 °C, 1 h, 1 MPa.

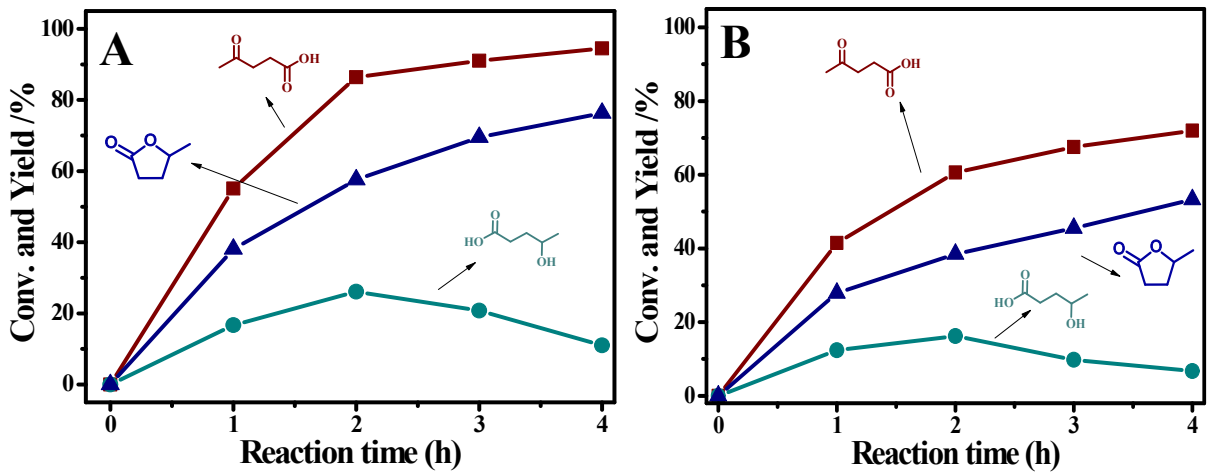

Fig. S37 Time resolved conversion and yield in $Ru_{1.5}$@TNph-PTA catalyzed conversion of LA into GVL at (A) 70 °C and (B) 50 °C. Reaction conditions: 1 mmol LA, 4 mL water, LA/Ru=350, 4 h, 1 MPa.

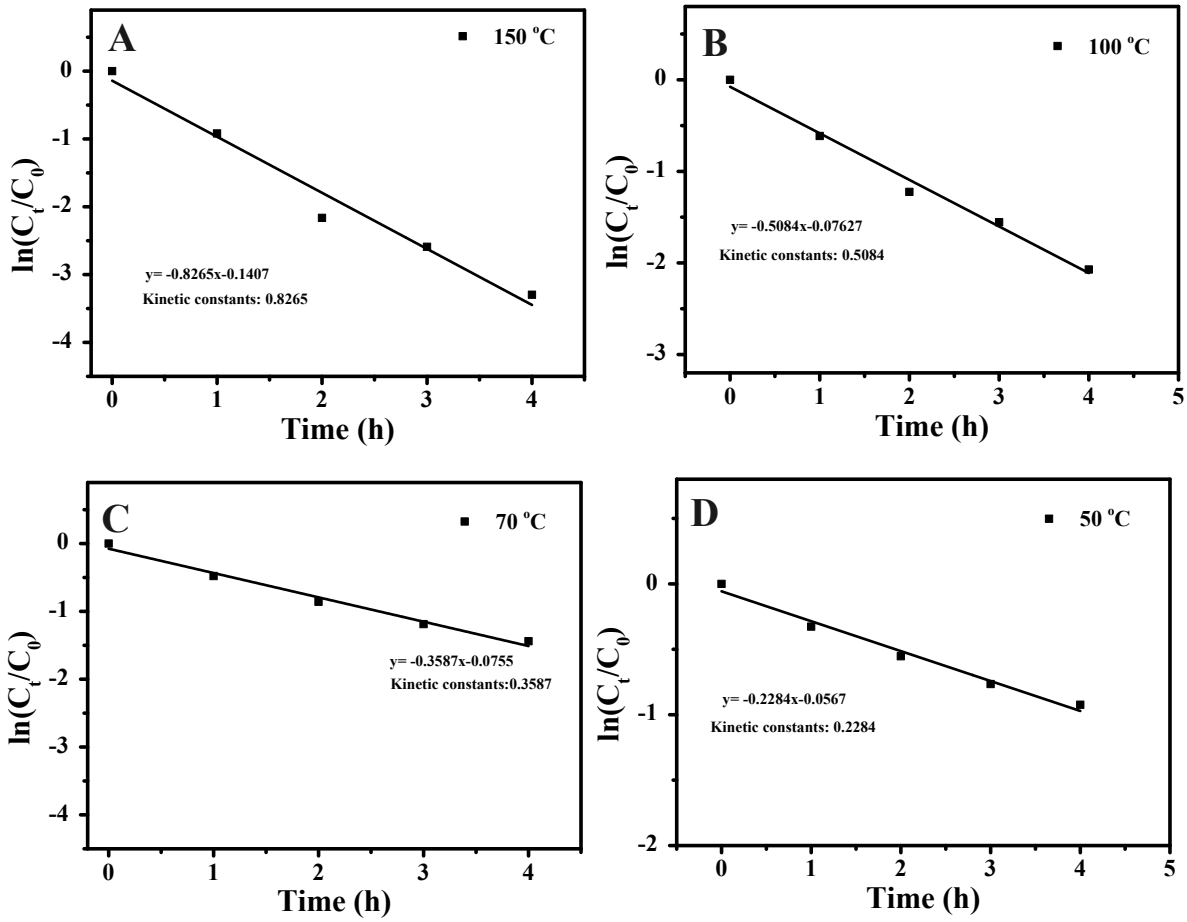

Fig. S38 Plots of $\ln(C_t/C_0)$*vs*. reaction time in $Ru_{1.5}$@TNph-PTA catalyzed conversion of LA into GVLat (A) 150 °C, (B) 100 °C, (C) 70 °C, (D) 50 °C.Reaction conditions: 1 mmol LA, 4 mL water, LA/Ru=350, 4 h, 1 MPa.

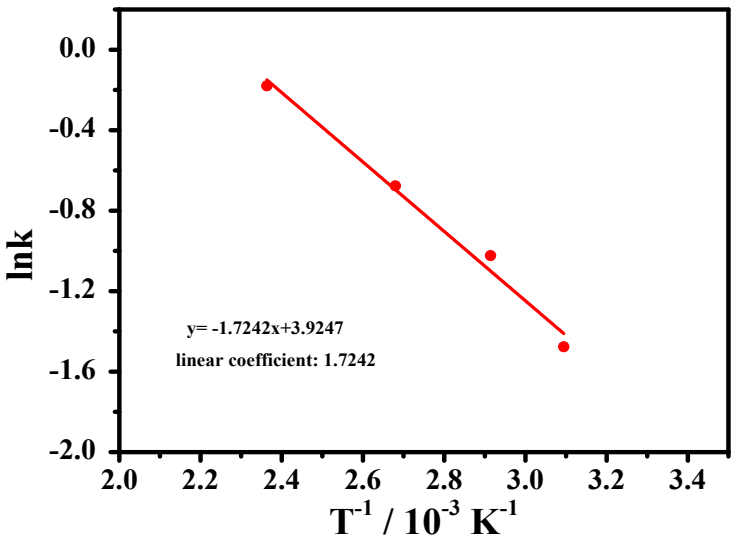

Fig. S39 Plots of ln(k) against T^{-1} for LA hydrogenation. Reaction conditions: 1 mmol LA, 4 mL water,LA/Ru=350, 4 h, 1 MPa.

Table S1. Element analyses

Entry	Sample	N %	C %	H %
1	DNph-PTA	16.51	47.90	5.37
2	$DNph_2$-PTA	14.84	56.38	7.10
3	TNph-PTA	13.89	54.18	3.98
4	TIph-PTA	8.45	53.94	4.23
5	TNph-PDA	10.95	51.31	3.65
6	TNph-TAPB	9.54	61.76	4.78
7	TNph-TAPM	11.30	55.99	5.48
8	$Ru_{1.5}$@TNph-PTA	13.41	54.09	3.81

Table S2. Synthetic conditions and textural properties[a]

Entry	Solvent	Volume (mL)[b]	S_{BET}[c] (m^2 g^{-1})	Vp[d] (cm^3 g^{-1})	Dp[e] (nm)
1	NMP	15	122	0.61	20.1
2	DMF	15	25	0.10	15.6
3	DMF/NMP	10/10	150	0.78	20.8
4	DMF/NMP	5/10	94.2	0.45	19.2
5	DMF/NMP	10/5	47.7	0.22	18.8
6	THF/NMP	10/10	26.1	0.09	13.4
7	TMB/NMP	10/10	42.4	0.31	29.1

[a]iMPAs synthesized through the condensation of TNph and PTA by using different solvents. Synthesis condition: TNph 0.8 mmol, PTA 0.6 mmol, $SOCl_2$ 1.7 mmol, TEA 1 mmol, 140 ^oC, 24 h. [b]Solvent volume in the synthesis system. [c]BET surface area. [d]Total pore volume. [e]Average pore diameter.

Table S3. Synthetic conditions and textural properties[a]

Entry	Reaction time (h)	Production yield (%)	S_{BET}[b] (m^2 g^{-1})	Vp[c] (cm^3 g^{-1})	Dp[d] (nm)
1	3	19.4	1.4	-	-
2	6	50.3	18	0.135	29.3
3	12	58.3	22	0.07	13.3
4	24	61.1	150	0.78	20.8

[a]iMPAs synthesized through the condensation of TNph and PTA by different polymerization time. [b]BET surface area. [c]Total pore volume. [d]Average pore diameter.

Table S4. Textural properties

Entry	Sample	Ru (wt%)	S_{BET}[a] (m^2 g^{-1})	Vp[b] (cm^3 g^{-1})	Dp[c] (nm)
1	$Ru_{0.5}$@TNph-PTA	0.51	84	0.56	15.3
2	Ru_5@TNph-PTA	3.82	60	0.31	13.9
3	Ru_8@TNph-PTA	5.68	49	0.29	12.7
4	Ru/C	5	808	0.41	2
5	TNph-PTA-N	-	5	0.02	-
6	$Ru_{1.5}$@TNph-PTA-N	1.25	3	0.01	-
7	TA-PTA	-	80	0.61	30.2
8	$Ru_{1.5}$@TA-PTA	1.23	69	0.54	26.5
9	PDMBr	-	121	0.68	22.4
10	$Ru_{1.5}$@PDMBr	1.62	94	0.51	15.9
11	Reused $Ru_{1.5}$@TNph-PTA	1.44	85	0.39	14.8

[a]BET surface area. [b]Total pore volume. [c]Average pore diameter.

Table S5. Dispersion and specific active surface area of Ru in catalysts

	Dispersion (%)	**Ru metal S. A. (m^2 g^{-1})[a]**	**Average particle size (nm)**	**GVL (%)**	**Yield**
$Ru_{0.5}$@TNph-PTA	37	134.2	1.71	97.8	
$Ru_{1.5}$@TNph-PTA	35	126.9	1.82	96.3	
Ru_5@TNph-PTA	31	112.4	2.15	94.5	
Ru_8@TNph-PTA	29	105.1	2.07	93.7	
$Ru_{1.5}$@TNph-PTA-N	23	83.4	3.21	64.8	
$Ru_{1.5}$@PDMBr	28	101.5	2.48	87.4	
$Ru_{1.5}$@TA-PTA	25	90.7	2.60	70.5	
Ru/C	16	59.9	12.3	43.8	
Reused $Ru_{1.5}$@TNph-PTA	33	119.7	2.08	94.3	

[a]specific active surface area of Ru.

Table S6. The surface chemical state of Ru species and the proportion of Ru(0)

		$Ru_{1.5}$@TNph-PTA	$Ru_{1.5}$@PDMBr	$Ru_{1.5}$@TA-PTA	Ru/C
B.E. (eV)	Ru(0)	484.4/462.2	484.4/462.2	484.4/462.2	484.4/462.2
	Ru(III)	486.3/464.1	486.3/464.1	486.3/464.1	486.3/464.1
	$A_{(Ru(0))}/A_{(Ru(III))}$	70.7%/29.3%	62.1%/37.9%	54.5%/45.5%	38.9%/61.1%

Table S7. Hydrogenation of LA into GVL[a]

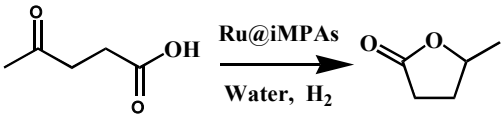

Entry	Samples	Ru wt%	Particle size (nm)	Conv. (%)	Yield (%)	TON[b]	TOF[c] (h^{-1})	STY[d]
1	Ru/C	5.00	12.3	21.7	8.5	297	891	51.7
2	Ru_8@TNph-PTA	5.68	2.07	48.3	21.4	749	2247	148
3[e]	Ru/C	5.00	12.3	15.9	5.6	979	2937	170
4[e]	Ru_8@TNph-PTA	5.68	2.07	29.2	11.9	2082	6246	411

[a]Reaction conditions: 10 mmol LA, 4 mL water, LA/Ru=3500, 150 °C, 20 min, 1 MPa. [b]Turnover number (TON) = mol GVL obtained)/(mol Ru). [c]Turnover frequency (TOF) = (mol GVL obtained)/(mol Ru × h). [d]Space time yield (STY) = (g GVL obtained)/(gcatalyst × h). [e]50 mmol LA (LA/Ru=17500).

Table S8. Comparison of supported catalysts in hydrogenation of LA to GVL

Entry	Catalysts	Ru (wt%)	T (°C)	H_2 (MPa)	Solvent	Yield[a]/Yield[b]	TOF[c]	STY[d] (g_{GVL} $g_{catalyst}^{-1}$ h^{-1})	Ref.
1	Ru-Pd/TiO_2	1.0	200	4.0	1,4-dioxane	99.6/-	2160	-	S1
2	Ru/ZrO_2	1.0	150	3.0	γ-octalactone	100/94.3	936	3.83	S2
3	2RuAl-SEA	2.0	220	1.38	1,4-dioxane	-/-	2484	4.06	S3
4	0.300Ru-CNF	0.27	150	4.5	solvent-free	95/62	956	3.13	S4
5	Ru/ZrO_2@C	0.85	140	1.0	water	96.4/88.4	482	2.35	S5
6	Ru-HAP	4.9	70	0.5	water	99/89	14.9	5.00	S6
7	Ru/MIL-101(Cr)	5.0	70	1.0	water	86/52	71.6	4.40	S7
8	Ru/SMS	4.6	70	0.5	water	95.6/-	50	0.66	S8
9	Ru/Mg–LaO	5.0	130	1.2	water	99/-	87	4.52	S9
10	$Ru_{1.5}$@TNph-PTA	1.46	150	1.0	water	96.3/94.3	84.3	1.42	This work
	Ru_8@TNph-PTA	5.46				98.8/-	462	19.0/411[e]	

[a]Yield of the fresh catalyst. [b]Yield of the spent catalyst after several recycling runs and "-" means that the reusability was currently unclear. [c]Turnover frequency (TOF) = mol GVL/(mol Ru × h). [d]Space time yield =g GVL/(gcatalyst × h). [e]under reaction time of 20 min.

Details for the comparison of Ru catalysts in LA conversion to GVL

Table S8 lists the reaction conditions and catalytic performance of typical efficient Ru-based catalysts in the hydrogenation of LA into GVL. Though directly comparing the catalytic performances of different catalysts is difficult because of the variation of the reaction conditions (substrate amount, solvent, pressure, temperature, etc.), reasonable comparison can be made by comprehensively considering the activity (conversion, yield, TOF and STY etc.) and stability under similar reaction conditions. Various supported Ru and Ru alloy NPs exhibited high efficiency by using organic solvent or under solvent-free condition. However, the recycling performance of many systems was unclear or suffered from apparent deactivation. Noticeably, Ru NPs on iMPAs in this work maintained the activity in a five-run test under both saturated conversion (Fig. 5A) and moderate conversion (Fig. S31), which is additionally reflected by the almost identical kinetic curve of $Ru_{1.5}$@TNph-PTA in the 5th run to that in the 1st run (Fig. S32) plus the calculation of the cumulative TON and average TOF (Table S9 and S10, as seen below). Particularly, the combination of robust Ru NPs and high loading over the catalyst Ru_8@TNph-PTA (5.68 wt%) endow both high yield, turnover frequency (TOF) and space time yield (STY). The STY value was 19.0 $g_{GVL}\ g_{catalyst}^{-1}\ h^{-1}$under complete conversion (>99) and dramatically increased to be 411$g_{GVL}\ g_{catalyst}^{-1}\ h^{-1}$within the initial stage (conversion: 30%, reaction time: 20 min), significantly exceeding previous ones under similar conditions. Besides, the reaction occurred under relatively low H_2 pressure and by using water the solvent that is favorable from the green and sustainable perspective. The comparison above indicates that Ru NPs iMPAs in this work serves as the effective and stable heterogeneous catalyst for hydrogenation of LA to GVL.

Table S9. Recycling of $Ru_{1.5}$@TNph-PTA in hydrogenation of LA into GVL

Run	Yield	TON	Cumulative TON	Average TOF
1	96.3	337	337	84.3
2	95.5	334	671	83.9
3	95.7	335	1006	83.8
4	95.1	333	1339	83.7
5	94.3	330	1669	83.5

Reaction conditions: 1 mmol LA, 4 mL water, LA/Ru=350, 4 h, 1 MPa, 150 °C.

Table S10. Recycling of $Ru_{1.5}$@TNph-PTA in hydrogenation of LA into GVL

Run	Yield	TON	Cumulative TON	Average TOF
1	76.2	259	259	64.7
2	75.7	257	516	64.5
3	75.4	257	773	64.4
4	75.1	256	1029	64.3
5	75.3	256	1285	64.3

Reaction conditions: 1 mmol LA, 4 mL water, LA/Ru=350, 4 h, 1 MPa, 70 °C.

Table S11. Calculation of minimized energy

Object	Structureformula	Optimized configuration	Minimized energy (kcal mol^{-1})
TNph-PTAunit (Model I)	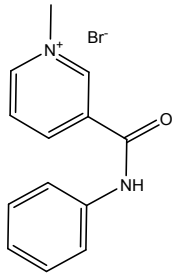	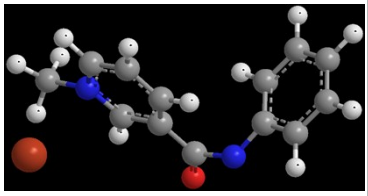	Stretch: 0.8239 Bend: 3.4592 Stretch-Bend: 0.1374 Torsion:1.7683 Non-1,4VDW: 4.5152 1,4 VDW: 14.9770 Charge/Charge:-72.2915 Charge/Dipole: 2.4331 Dipole/Dipole: -6.7552 **TotalEnergy:-50.9327 kcal mol^{-1}**
TNph-PTAunit +Ru	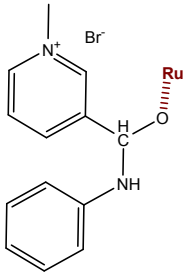	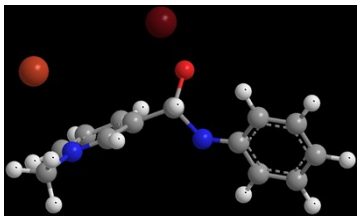	Stretch: 1.1127 Bend: 4.4123 Stretch-Bend: 0.2434 Torsion: -10.0539 Non-1,4 VDW: 1.8860 1,4 VDW: 17.8202 Charge/Charge: -72.6749 Charge/Dipole: -0.4884 Dipole/Dipole: 1.9526 **Total Energy: -55.7900 kcal mol^{-1}**
PDMBr unit (Model II)	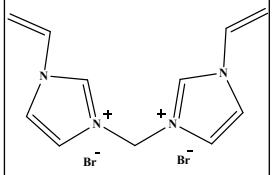	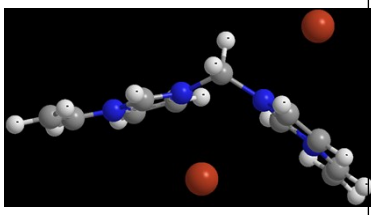	Stretch: 0.9580 Bend: 28.2796 Stretch-Bend: 0.0083 Torsion: -1.2943 Non-1,4 VDW: 25.3578 1,4 VDW: 6.5745 Charge/Charge: -267.5262 Charge/Dipole: -6.7967 Dipole/Dipole: 0.0143 **Total Energy: -214.4247 kcal mol^{-1}**
PDMBr unit + Ru	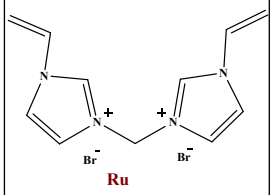	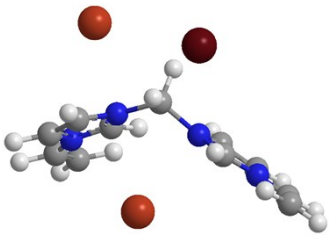	Stretch: 0.9522 Bend: 28.2855 Stretch-Bend: 0.0055 Torsion: -1.3030 Non-1,4 VDW: 23.7017 1,4 VDW: 6.5708 Charge/Charge: -267.5271 Charge/Dipole: -6.7760 Dipole/Dipole: 0.0142 **Total Energy: -216.0761 kcal mol^{-1}**

TA-PTA unit (Model III)	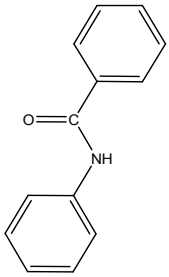	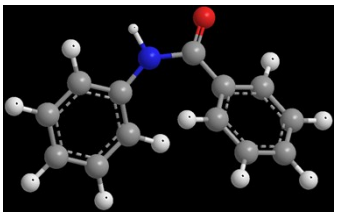	Stretch: 0.5737 Bend: 6.5607 Stretch-Bend: 0.0658 Torsion: 0.3964 Non-1,4 VDW: 0.2506 1,4 VDW: 9.7154 Dipole/Dipole: -9.4292 **Total Energy: 8.1335 kcal mol^{-1}**
TA-PTA unit +Ru	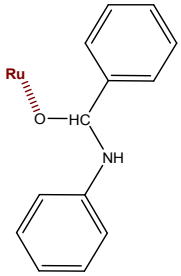	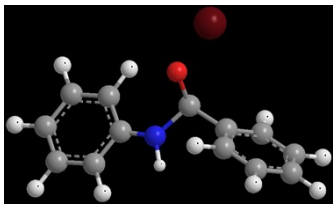	Stretch: 0.9205 Bend: 4.0620 Stretch-Bend: 0.1722 Torsion: -13.5249 Non-1,4 VDW: -3.0473 1,4 VDW: 16.0513 Dipole/Dipole: 1.3947 **Total Energy: 6.0284 kcal mol^{-1}**

Table S12. Total minimized energy and stabilization energy

Object	**TNph-PTA (kcal mol^{-1})**		**PDMBr (kcal mol^{-1})**		**TA-PTA (kcal mol^{-1})**	
	MTE	SE	MTE	SE	MTE	SE
RUS	-50.9327	-	-214.4247	-	8.1335	-
RUS + Ru	-55.7900	-4.5873	-216.0761	-1.6514	6.0284	-2.1051

REFERENCE

S1 W. Luo, M. Sankar, A. M. Beale, Q. He, C. J. Kiely, P. C. A. Bruijnincxand M. Weckhuysen, *Nat. Commun.,* 2015, **6**, 6540–6549.

S2 J. Ftouni, A. Munoz-Murillo, A. Goryachev, J. P. Hofmann, E. J. M. Hensen, L. Lu, C. J. P. Kiely, C. A. Bruijnincx and B. M. Weckhuysen, *ACS Catal.,* 2016, **6**, 5462–5472.

S3 S. Cao, J. R. Monnier and J. R. Regalbuto, *J. Catal.,* 2017, **347**, 72–78.

S4 Y. Yang, C. J. Sun, D. E. Brown, L. Q. Zhang, F. Yang, H. R. Zhao, Y. Wang, X. H. Ma, X. Zhang, and Y. Ren, *Green Chem.,* 2016, **18**, 3558–3566.

S5 W. Cao,W. Luo, H. Ge, Y. Su, A. Wang and T. Zhang, *Green Chem.,* 2017, **19**, 2201–2211.

S6 M. Sudhakar, K. M. Lakshmi, J. V. Swarna, R. Kishore, K. V. Ramanujachary and A. Venugopal, *Catal. Commun.,* 2014, **50**, 101–104.

S7 Y. Guo, Y. Li, J. Chen, and L. Chen, *Catal. Lett.,* 2016, **146**, 2041–2052.

S8 Y. Kuwahara, Y. Magatani and H. Yamashita, *Catal. Today,* 2015, **258**, 262–269.

S9 J. V. Swarna, M. Sudhakar, K. S. Naveen and A. Venugopal, *RSC Adv.,* 2015, **5**, 9044–9049.